

VRIJE UNIVERSITEIT AMSTERDAM  
JULY 2025

---

# Tail Risk Dependencies in East Asian Markets: A GARCH-EVT-Copula Approach Focused on the Korean Market

---

Master Thesis of Financial Econometrics

THESIS COMMISSION:

ERAN RAVIV (SUPERVISOR)

LENNART HOOGERHEIDE (CO-READER)

YUNJI Eo (2735445)



August 17, 2025

## Abstract

This study explores the dependencies of tail risk in East Asian financial markets centered on the Korean market by using a GARCH-EVT-Copula approach. The methodology integrates GARCH models for volatility filtering, Extreme Value Theory (EVT) for tail behavior modeling, and vine copulas to capture dependence structures. The analysis focuses on daily returns from the KOSPI, S&P 500, SSE, and Nikkei 225 from 2014 to 2024. Results show significant fat tails across all assets and strong lower tail dependence between the KOSPI and other markets. The proposed framework outperforms traditional risk measures, with the EGARCH-EVT-Copula model demonstrating superior Value-at-Risk backtesting accuracy.

**Keywords:** Tail risk, Extreme Value Theory, Copula, GARCH, East Asian markets, Value-at-Risk

## 1 Introduction

“It does not matter how frequently something succeeds if failure is too costly to bear.” Nassim Nicholas Taleb, *The Black Swan* (Taleb, 2007). This quote articulates the critical perspective on tail risk: rare events, though low in probability, can have catastrophic consequences, as illustrated by crises like the 2008 global financial crisis and the COVID-19 pandemic. Asian markets, including South Korea and China, are particularly exposed to such risks due to higher volatility, as seen in the 2015–2016 Chinese market crash, underscoring the need to understand tail events and their dependencies for effective risk management. However, traditional risk measures often fail to capture extreme events due to normality assumptions and neglect of fat tails and asymmetric dependencies. While GARCH models capture volatility clustering, they are limited in describing extreme values, whereas Extreme Value Theory (EVT) explicitly models tail behavior, and copula methods capture complex market dependencies. Combining these methods enables a comprehensive examination of tail risks across markets. This study applies a GARCH-EVT-Copula framework to analyze and compare the tail risk structures of major Asian stock markets, focusing on South Korea, China, and Japan, with the US market as a benchmark, with particular attention to the Korean market’s relationships with other regional markets to understand tail risk dynamics in East Asia.

The paper is structured as follows. Section 2 reviews the relevant literature on tail risk modeling. Section 3 describes the data and preliminary analysis. Section 4 details the GARCH-EVT-Copula methodology for modeling marginals, dependencies, and VaR. Section 5 presents empirical results, including GARCH fitting, EVT estimates, copula fitting, and VaR backtesting. Section 6 concludes with key findings and future research directions. Additionally, Appendix A presents Stochastic Volatility models with normal distribution assumptions as an alternative perspective on tail risk modeling.

## 2 Literature Review

Tail risk is defined as the financial risk of an asset or portfolio of assets moving more than three standard deviations from its current price, above the risk of normal distribution. Traditional portfolio strategies rely heavily upon the assumption that market returns follow a normal distribution, characterized by the bell curve, which illustrates that, given enough observations, all values in a sample will be distributed symmetrically with respect to the mean. The most standard measure of tail risk is Value-at-Risk (VaR), which is widely used in the finance due to its ease of interpretation and applicability. However, despite its popularity, VaR has faced significant criticism. For instance, prominent critic Nassim Taleb notably argued that VaR was fundamentally flawed in its claims to estimate the risks of rare, extreme events, often leading to a false sense of security.

In fact, financial markets are not perfect, as they are largely shaped by unpredictable human behavior, and the distribution of returns is, in fact, not normal, but skewed. Early studies by [Mandelbrot \(1963\)](#) and [Black \(1976\)](#) documented that financial returns exhibit fat tails and clustering of volatility, violating the assumption of normality. When observed tails are fatter than traditionally predicted, this can result in significant fluctuations in the value of the stock, which subsequently tends to underestimate volatility and risk of the asset. The importance of considering tail risk in portfolio management is not only theoretical. [McRandall and Rozanov \(2012\)](#) observe that in the period from the late 1980s to the early 2010s, there were at least seven episodes that can be viewed as tail events: the equity market crash of 1987, the 1994 bond market crisis, the 1997 Asian financial crisis, the 1998 Russian financial crisis and the Long-Term Capital Management blow-up, the dot-com bubble collapse, the subprime mortgage crisis, and the infamous Bankruptcy of Lehman Brothers.

While traditional VaR struggles with non-normal financial data, advancements in volatility modeling have offered significant improvements in capturing the nature of financial markets. The Generalized Autoregressive Conditional Heteroskedasticity (GARCH) model, proposed by [Bollerslev \(1986\)](#), became a standard model for volatility clustering. Building upon this, extensions like the Glosten-Jagannathan-Runke GJR-GARCH model ([Glosten et al., 1993](#)), and the Exponential GARCH model developed by [Nelsen \(2006\)](#), were introduced to further capture asymmetric effects, also known as the leverage effect, where negative shocks lead to greater volatility than positive shocks of the same magnitude. These models have significantly enhanced the accuracy of volatility forecasts for financial returns. Despite these improvements of handling volatility by GARCH family models, they often lack addressing the extreme tail behavior of return distributions. This inherent limitation becomes critical when managing tail risk, where the focus is precisely on these extreme events.

To overcome these challenges, Extreme Value Theory (EVT) has emerged as a powerful statistical framework specifically designed for modeling the behavior of extreme observations. Rather than attempting to model the entire data distribution, EVT focuses exclusively on the tails, allowing for more accurate estimations of extreme quantiles. The theoretical foundations of EVT were established by [Gnedenko \(1943\)](#) and unified under the Generalized Extreme Value (GEV) distribution by [Gumbel \(1958\)](#). A common and efficient approach within EVT is the Peaks-Over-Threshold (POT) method, proposed by [Pickands \(1975\)](#) and further developed by [Balkema and De Haan \(1974\)](#), which models exceedances over a high threshold using the Generalized Pareto Distribution (GPD). By first filtering returns with a volatility model like GARCH and then applying EVT to the standardized residuals, these combined approaches can account for both volatility clustering and the precise behavior of extreme events. For instance, [Xiao \(2024\)](#) developed an SV-EVT model, and [Chebbi and Hedhli \(2022\)](#) proposed a GARCH-EVT-Copula approach, both demonstrating through backtesting that such integrated models are more effective for VaR estimation than traditional methods, as they better capture the fat-tailed properties and leverage effects of financial returns.

Beyond modeling the tails of individual assets, capturing the dependence between markets is crucial, especially during periods of stress when markets move together. For example, the COVID-19 pandemic, during which global markets experienced simultaneous declines, highlights the importance of modeling these dependencies to understand systemic risk. To address this need, copula theory ([Sklar, 1959](#)) offers a flexible framework for modeling complex dependence structures by separating marginal behaviors from the dependence structure itself. This approach enables the capture of non-linear and asymmetric relationships that frequently occur during extreme market conditions. Given that this paper examines four markets, vine copulas ([Aas et al., 2009a](#)) are particularly suitable, as they construct multidimensional copulas through sequences of bivariate trees, allowing for a detailed analysis of cross-market dependencies.

Integrating copulas with EVT and GARCH models has proven effective in capturing extreme co-movements and measuring tail risk more accurately. For instance, [Chebbi and Hedhli \(2022\)](#) demonstrated that a GARCH-EVT-C-vine copula approach outperforms traditional VaR methods in the MENA markets. Similarly, [Hsu et al. \(2012\)](#) found that combining the Clayton copula with EVT improves risk measurement for Asian markets, while [Zhang et al. \(2014\)](#) showed that vine copulas enhance the capture of tail dependencies during financial crises.

While [Park and Lee \(2022\)](#) examined asymmetric tail dependence using GPD and copulas and analyzed the Korean market, their study primarily focused on portfolio optimization across global markets, including the US, Europe, and Asia, and applied EVT directly to raw returns without accounting for volatility clustering, potentially violating the i.i.d. assumption required by EVT. In contrast, this

study employs a GARCH-EVT-Copula framework that first filters volatility dynamics with GARCH, then applies EVT to the standardized residuals, and finally captures tail dependencies using vine copulas. This three-stage approach ensures the proper application of EVT while simultaneously modeling volatility clustering and complex dependence structures. Building on these developments, this study specifically examines tail risk dependencies within East Asia, focusing on the Korean market and its relationships with China, Japan, and the US. This Korea-centered approach aims to understand how extreme events are related across East Asian markets, providing insights into the regional transmission of tail risks, particularly given Korea's role as a regional financial hub.

### 3 Data Analysis

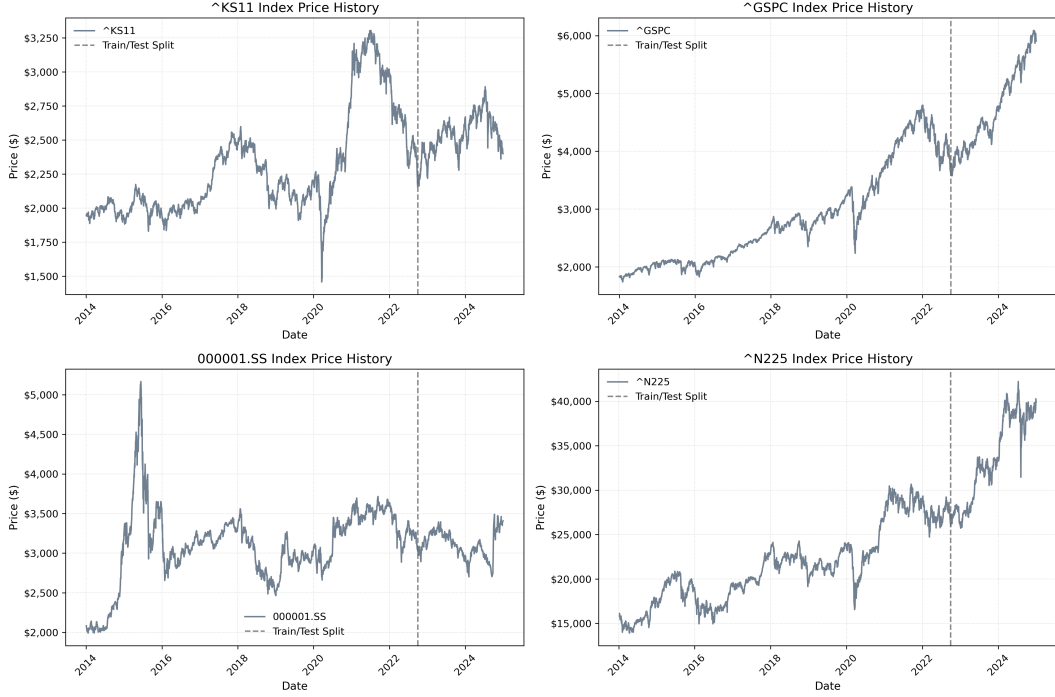


Figure 1: KOSPI, S&P 500, SSE, Nikkei 225: Price Trends (2014–2024)

Note: The sample spans 2014–2024. The dashed line marks the train-test split. Ticker symbols:  $^{\wedge}\text{KS11}$  (KOSPI),  $^{\wedge}\text{GSPC}$  (S&P 500),  $000001.\text{SS}$  (SSE),  $^{\wedge}\text{N225}$  (Nikkei 225).

This paper focuses on four markets: KOSPI (South Korea), S&P 500 (United States), SSE Composite (China), and Nikkei 225 (Japan), which are the representative stock indices for their respective countries. The main focus of this thesis is tail risk analysis centered on the Korean market, for which KOSPI is selected as the primary indicator. The SSE Composite and Nikkei 225 are included due to the strong economic and financial relationships between China, Japan, and South Korea, while the S&P 500 is used as a benchmark to reflect the influence of the US market on global financial dynamics. The dataset comprises daily prices from January 2014 to December 2024 and is partitioned into training (January 2014 to September 2022) and testing (October 2022 to December 2024) periods to evaluate model performance. For the return analysis, the dataset was aligned using common trading dates across all four indices to ensure consistency, while the price trends are presented over the entire available period for each market.

Figure 1 illustrates the price trends of the selected indices over the sample period. During this period, several significant extreme events occurred. The SSE experienced a sharp rise followed by an immediate crash due to the Chinese stock market bubble burst in 2015. The KOSPI showed a substantial decline in 2022, driven by a combination of global monetary tightening, inflation concerns, and geopolitical tensions, including the Russia-Ukraine conflict. Furthermore, the data exhibit common downward movements across all four markets, with the most notable example being the COVID-19

market crash in early 2020, where the KOSPI, S&P 500, and Nikkei 225 experienced simultaneous sharp declines. After the train-test split in late 2022, the KOSPI and SSE exhibited gradual downward trends, while the S&P 500 and Nikkei 225 showed upward movements during the same period.

Instead of using actual prices, log returns are employed to focus on the rate of change. Log returns are defined as follows:

$$r_t = \log(P_t) - \log(P_{t-1}) \quad (1)$$

where  $P_t$  represents the closing price at time  $t$ .

Table 1: Summary Statistics of Log Returns for Train/Test Period

	<b>KOSPI</b>		<b>S&amp;P 500</b>		<b>SSE</b>		<b>Nikkei 225</b>	
	Train	Test	Train	Test	Train	Test	Train	Test
Mean (%)	0.007	-0.022	0.042	0.081	0.013	0.016	0.026	0.055
Std Dev (%)	0.992	1.135	1.143	0.925	1.358	0.992	1.281	1.380
Skewness	-0.471	-0.871	-1.088	0.228	-0.982	1.509	-0.106	-1.382
Kurtosis	8.689	9.425	18.821	2.659	7.521	9.210	4.314	22.766
Min (%)	-8.77	-9.18	-12.77	-3.04	-8.87	-3.11	-8.25	-13.23
Max (%)	8.25	5.50	8.97	5.40	6.04	7.76	7.73	9.74
JB Stat	5969***	1811***	28066***	143***	4723***	1854***	1457***	10380***

Note: \*\*\* indicates statistical significance at the 1% level. All JB statistics reject the null hypothesis of normality.

With these transformed data, which are log-returns, the distributional characteristics of each dataset can be examined through summary statistics. Table 1 presents the summary statistics of log returns for both the training and test periods. Several important observations emerge from this analysis. First, most datasets exhibit negative skewness, except for the test data of the S&P 500 and the SSE, indicating that downside tail risks are relatively greater. Second, all datasets, except for the test data of the S&P 500, display kurtosis values substantially exceeding 3, the benchmark for a normal distribution. This observation is further confirmed by the Jarque-Bera statistics, which are highly significant across all datasets, providing strong evidence that returns are not normally distributed but instead exhibit fat tails. Finally, most of the datasets show a clear asymmetry between extreme losses and gains, with maximum losses exceeding maximum gains in absolute terms, aligning with the negative skewness observed. These findings underscore the limitations of assuming normality when modeling financial returns, particularly in capturing the extreme movements and tail risks observed in the data.

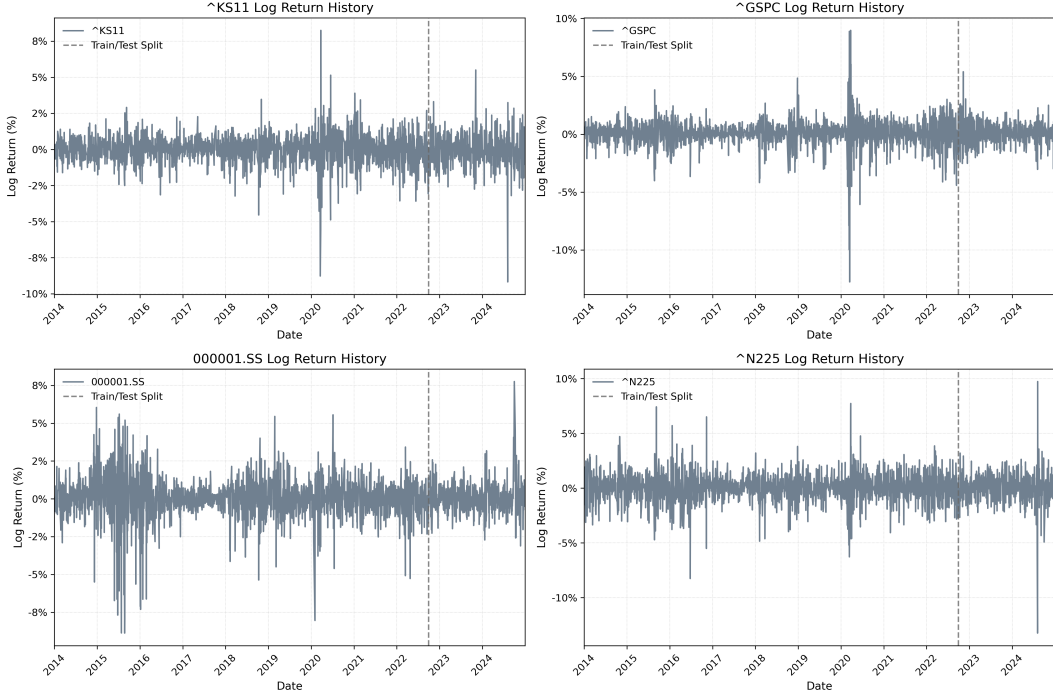


Figure 2: KOSPI, S&P 500, SSE, Nikkei : Log-return Series (2014-2024)

Note: The sample spans 2014–2024. The dashed line marks the train-test split. Ticker symbols:  $\wedge\text{KS11}$  (KOSPI),  $\wedge\text{GSPC}$  (S&P 500),  $000001.\text{SS}$  (SSE),  $\wedge\text{N225}$  (Nikkei 225).

Figure 2 visually complements the summary statistics by illustrating the log-return series for the selected indices over the sample period. Volatility clustering and extreme spikes are clearly observable, particularly during periods of market stress such as the COVID-19 crisis. Building upon these empirical findings, the following section details the methodological framework employed to model tail risks and dependencies using GARCH filtering, EVT, and copula approaches.

## 4 Methodology

This section outlines the comprehensive framework for constructing and evaluating multivariate risk models that combine GARCH models, Extreme Value Theory, and copula-based dependence structures. The analysis proceeds in four integrated stages. First, the marginal distributions of individual asset returns are modeled using GARCH family models to filter out volatility clustering and obtain standardized residuals. Second, Extreme Value Theory is applied to these residuals using a semi-parametric approach that combines Generalized Pareto distributions for the tails with empirical methods for the interior, ensuring accurate representation of extreme events. Third, C-vine copulas are utilized to capture the dependence structure between assets, allowing for flexible modeling of non-linear and asymmetric dependencies. Finally, Value at Risk calculations are implemented through Monte Carlo simulation, and model performance is evaluated against established benchmarks.

### 4.1 Marginal Distribution Modeling

The first step involves modeling the marginal distributions of individual asset returns. This section outlines the process of extracting standardized residuals from GARCH family models and subsequently transforming them into uniform variables using EVT. This transformation is essential for the copula-based dependence modeling that follows.

## 4.2 GARCH Family Models

Accurate volatility estimation is crucial for applying Extreme Value Theory, as EVT requires independently and identically distributed (i.i.d.) data. Applying EVT directly to raw returns would violate this assumption due to the presence of volatility clustering. To address this issue, GARCH family models are employed to filter returns and extract standardized residuals, as these models have become the standard approach in financial econometrics for capturing time-varying volatility while maintaining computational efficiency. Additionally, based on the results from the data analysis, which indicate the rejection of the normality assumption in return distributions, a Student-t distribution is adopted within the GARCH models to better capture the observed heavy tails.

### GARCH

GARCH(p,q) model proposed by [Bollerslev \(1986\)](#) is defined as following :

$$\begin{aligned} r_t &= \sigma_t \epsilon_t, \\ \sigma_t^2 &= \omega + \sum_{i=1}^q \alpha_i r_{t-i}^2 + \sum_{j=1}^p \beta_j \sigma_{t-j}^2 \end{aligned} \quad (2)$$

where  $\sigma_t^2$  is the conditional variance, and  $r_{t-i}^2$  are the past squared errors from the return.

In this paper, we use a first lag for the conditional variance and the past squared errors. Hence, the parameter restrictions for GARCH(1,1) are defined as following :

$$\begin{aligned} \sigma_t^2 &= \omega + \alpha \epsilon_{t-1}^2 + \beta \sigma_{t-1}^2 \\ \theta &= (\mu, \omega, \alpha, \beta) \\ \omega > 0, \alpha &\geq 0, \beta \geq 0, \alpha + \beta < 1 \end{aligned} \quad (3)$$

### GJR-GARCH

Proposed by [Glosten et al. \(1993\)](#), Jagannathan, and Runkle , the Glosten-Jagannathan-Ranke GJR-GARCH is presented as follows :

$$\begin{aligned} r_t &= \sigma_t \epsilon_t, \\ \sigma_t^2 &= \omega + \sum_{i=1}^q (\alpha_i + \gamma_i I_{t-i}) r_{t-i}^2 + \sum_{j=1}^p \beta_j \sigma_{t-j}^2, \\ I_{t-i} &= \begin{cases} 1 & \text{if } r_{t-i} \leq 0, \\ 0 & \text{otherwise} \end{cases} \end{aligned} \quad (4)$$

The model incorporates asymmetry in the volatility process described by the parameter  $\gamma$ . When  $\gamma > 0$ , the model captures the leverage effect, where negative shocks to returns lead to higher volatility than positive shocks of the same magnitude. When  $\gamma = 0$ , the GJR-GARCH model reduces to GARCH model. For  $\gamma < 0$ , the negative shocks result in smaller future volatility.

For the GJR-GARCH(1,1), the parameter restrictions are defined as :

$$\begin{aligned} \sigma_t^2 &= \omega + \alpha r_{t-1}^2 + \beta \sigma_{t-1}^2 + \gamma I_{[r_{t-1} < 0]} r_{t-1}^2, \\ \theta &= (\mu, \omega, \alpha, \beta, \gamma), \\ \omega > 0, \alpha &\geq 0, \beta \geq 0, \omega + \alpha + \beta + \gamma E[I_{[r_{t-1} < 0]}] < 1 \end{aligned} \quad (5)$$

### EGARCH

The Exponential Generalized Autoregressive Conditional Heteroskedasticity (EGARCH) model developed by [Nelson \(1991\)](#) is an extension of the GARCH model that captures asymmetry and leverage effects:

$$r_t = \sigma_t \epsilon_t,$$

$$\log(\sigma_t^2) = \omega + \sum_{i=1}^p \alpha_i \left| \frac{r_{t-i}}{\sigma_{t-i}} \right| + \sum_{j=1}^q \beta_j \log(\sigma_{t-j}^2) + \sum_{k=1}^r \gamma_k \frac{r_{t-k}}{\sigma_{t-k}}, \quad (6)$$

where the shock is asymmetric for  $\gamma \neq 0$ , with an exponential leverage effect when  $\gamma < 0$  and a leverage effect when  $\gamma > 0$ . The logarithmic expression ensures that the volatility is always positive. The parameter restrictions for the EGARCH(1,1) model are as follows:

$$\begin{aligned} \log(\sigma_t^2) &= \omega + \alpha \left| \frac{r_{t-1}}{\sigma_{t-1}} \right| + \beta \log(\sigma_{t-1}^2) + \gamma \frac{r_{t-1}}{\sigma_{t-1}}, \\ \theta &= (\mu, \omega, \alpha, \beta, \gamma), \\ |\beta| &< 1. \end{aligned} \quad (7)$$

### 4.3 Extreme Value Theory

Having obtained standardized residuals from the GARCH models, the next step applies EVT to complete the marginal distribution modeling and to transform the data into uniform variables. This section introduces the Peaks-over-Threshold method and the semi-parametric approach used to construct the cumulative distribution function. The resulting uniform data on [0,1] serve as inputs for the copula analysis in the subsequent section.

#### 4.3.1 Peaks-over-Thresholds

There are two primary methods for conducting Extreme Value Theory (EVT): Block Maxima and Peaks-over-Thresholds (POT). Block Maxima uses only the maximum data from  $n$  observations, discarding the rest, which is often inefficient. Therefore, this paper employs the POT method. Its key idea is to analyze the behavior of all observations that exceed a reference level  $u$ , essentially utilizing all tail observations. Let  $X$  be a sequence of independent and identically distributed (i.i.d.) random variables with a Cumulative Distribution Function (CDF)  $F$ . Based on  $X$ , we can construct the distribution above the threshold, known as the Conditional Excess Distribution Function, defined as follows:

$$F_u = P\{X - u \leq y \mid X > u\} = \frac{F(y+u) - F(u)}{1 - F(u)}$$

Here,  $F$  describes the distribution of the time series  $X$ . The variable  $y$  represents the excesses of  $X$  over the threshold  $u$ , such that  $y \equiv X - u$ , where  $0 \leq y < X_F - u$ .  $X_F \leq \infty$  denotes the right endpoint of  $F$ . In this paper,  $X$  specifically refers to the sequence of standard residuals obtained from GARCH models. The exceedances,  $y$ , then follow the Generalized Pareto Distribution (GPD), defined as:

$$G_{\xi,\sigma}(y) = \begin{cases} 1 - \left(1 + \frac{\xi y}{\sigma}\right)^{-1/\xi} & \text{if } \xi \neq 0 \\ 1 - \exp\left(-\frac{y}{\sigma}\right) & \text{if } \xi = 0 \end{cases}$$

The GPD is characterized by its shape parameter ( $\xi$ ) and scale parameter ( $\sigma$ ). The shape parameter  $\xi$  determines the tail behavior: if  $\xi > 0$ , the distribution exhibits heavy tails (Fréchet type), where larger values of  $\xi$  indicate heavier tails and higher probability of extreme events. If  $\xi = 0$ , the distribution has exponential tails (Gumbel type), representing moderate tail behavior similar to the exponential distribution. If  $\xi < 0$ , the distribution has light tails with finite endpoints (Weibull type), implying a bounded maximum for the exceedances. The scale parameter  $\sigma$  controls the dispersion of the exceedances above the threshold.

#### 4.3.2 Semi-parametric CDF

To conduct copula analysis, uniform data is required. This can be achieved by applying the CDF transformation to the residuals. The CDF can be divided into three parts: upper tail, interior region, and lower tail. For the tail regions, POT theory is applied to fit the GPD and obtain the shape and scale

parameters. While one could choose the threshold by plotting the mean excess function, this paper uses the upper 90% and lower 10% quantiles as thresholds for the upper and lower tails respectively, for computational efficiency. For the interior region, the Empirical Cumulative Distribution Function (ECDF) is used. The complete semi-parametric CDF combines these three components to transform the standardized residuals into uniform random variables on [0,1], which are required for the subsequent copula modeling.

#### 4.3.3 Goodness-of-Fit Tests for GPD

To assess the adequacy of the GPD fit to the threshold exceedances, two goodness-of-fit tests are employed: the Cramér-von Mises test and the Anderson-Darling test. These tests evaluate how well the fitted GPD captures the empirical distribution of exceedances.

##### Cramér-von Mises ( $W^2$ ) Test

The Cramér-von Mises statistic measures the squared differences between the empirical and theoretical distribution functions:

$$W^2 = n \int_{-\infty}^{\infty} [F_n(x) - F_0(x)]^2 dF_0(x) \quad (8)$$

A lower  $W^2$  value indicates a better fit.

##### Anderson-Darling ( $A^2$ ) Test

The Anderson-Darling statistic incorporates a weighting function that emphasizes the tails of the distribution:

$$A^2 = n \int_{-\infty}^{\infty} \frac{[F_n(x) - F_0(x)]^2}{F_0(x)[1 - F_0(x)]} dF_0(x) \quad (9)$$

Similar to  $W^2$ , a lower  $A^2$  value suggests a better fit.

These two statistics are considered appropriate if they exhibit low values and correspond to high p-values. p-values are obtained through bootstrap resampling because of its computational efficiency. In this paper, the goodness-of-fit for GPD is assessed for both the lower and upper tails.

## 4.4 Dependence Structure Modeling

After transforming the marginal distributions to uniform variables, the next critical step is modeling the dependence structure between assets. According to Sklar's theorem [Sklar \(1959\)](#), any multivariate distribution can be decomposed into its univariate marginal distributions and a copula function that captures the pure dependence structure. This separation principle allows us to model complex dependencies independently from the marginal behaviors. Given that the portfolio used in this paper consists of 4 assets, vine copulas [Aas et al. \(2009b\)](#) are employed, which help to construct multidimensional copulas through a sequence of bivariate tree.

### 4.4.1 Copula Family Selection

The selection of appropriate copula families for each edge is crucial for accurately capturing the dependence structure. In this paper, the following copula families are considered :

- **Gaussian copula:**  $\Phi_\theta(\Phi^{-1}(u_1), \Phi^{-1}(u_2))$  — captures linear dependence with no tail dependence.
- **Gumbel copula:**  $\exp\left[-\left((- \log(u_1))^\theta + (- \log(u_2))^\theta\right)^{1/\theta}\right]$  — captures asymmetric dependence with upper tail dependence.
- **Rotated Gumbel copulas:**

$$- 90^\circ: u_2 - \exp\left[-\left((- \log(1 - u_1))^\theta + (- \log(u_2))^\theta\right)^{1/\theta}\right]$$

$$\begin{aligned}
& - 180^\circ: u_1 + u_2 - 1 + \exp \left[ - ((-\log(1-u_1))^\theta + (-\log(1-u_2))^\theta)^{1/\theta} \right] \\
& - 270^\circ: u_1 - \exp \left[ - ((-\log(u_1))^\theta + (-\log(1-u_2))^\theta)^{1/\theta} \right]
\end{aligned}$$

These rotations enable capturing lower or mixed tail dependence.

- **Clayton copula:**  $[\max\{u_1^{-\theta} + u_2^{-\theta} - 1; 0\}]^{-1/\theta}$  — captures asymmetric dependence with lower tail dependence.

- **Rotated Clayton copulas:**

$$\begin{aligned}
& - 90^\circ: u_2 - [\max\{(1-u_1)^{-\theta} + u_2^{-\theta} - 1; 0\}]^{-1/\theta} \\
& - 180^\circ: u_1 + u_2 - 1 + [\max\{(1-u_1)^{-\theta} + (1-u_2)^{-\theta} - 1; 0\}]^{-1/\theta} \\
& - 270^\circ: u_1 - [\max\{u_1^{-\theta} + (1-u_2)^{-\theta} - 1; 0\}]^{-1/\theta}
\end{aligned}$$

These rotations enable modeling upper or mixed tail dependence.

- **Frank copula:**  $-\frac{1}{\theta} \log \left[ 1 + \frac{(\exp(-\theta u_1) - 1)(\exp(-\theta u_2) - 1)}{\exp(-\theta) - 1} \right]$  — captures symmetric dependence without tail dependence.

- **Joe copula:**  $1 - [(1-u_1)^\theta + (1-u_2)^\theta - (1-u_1)^\theta(1-u_2)^\theta]^{1/\theta}$  — captures asymmetric dependence with strong upper tail dependence.

- **Rotated Joe copulas:**

$$\begin{aligned}
& - 90^\circ: u_2 - \left( 1 - [(u_1)^\theta + (1-u_2)^\theta - (u_1)^\theta(1-u_2)^\theta]^{1/\theta} \right) \\
& - 180^\circ: u_1 + u_2 - \left[ (u_1)^\theta + (u_2)^\theta - (u_1)^\theta(u_2)^\theta \right]^{1/\theta} \\
& - 270^\circ: u_1 - \left( 1 - [(1-u_1)^\theta + (u_2)^\theta - (1-u_1)^\theta(u_2)^\theta]^{1/\theta} \right)
\end{aligned}$$

These rotations allow capturing lower or mixed tail dependence.

- **Student-t copula:**  $T_{\theta_2}(T_{\theta_2}^{-1}(u_1), T_{\theta_2}^{-1}(u_2); \theta_1)$  — captures symmetric dependence with symmetric tail dependence, enabling modeling of joint extreme events.

For each edge in the vine structure, all candidate copula families are fitted, and the best-fitting one is selected based on the Akaike Information Criterion (AIC) or Bayesian Information Criterion (BIC). The rotated versions allow for the capture of different tail dependence patterns in various directions.

#### 4.4.2 C-vine Copula

A vine with  $d$  dimensions is represented by  $(d-1)$  trees. The tree  $j$  has  $(d+1-j)$  nodes and  $(d-j)$  edges. The edges of tree  $j$  become the following nodes of the tree  $(j+1)$ , and the nodes represent random variables with inverse distribution functions. For our sample of six markets, these two copulas are presented as follows.

$$f(x_1, x_2, x_3, x_4) = \begin{cases} = f_1 f_2 f_3 f_4 \\ \times c_{12}(F_1, F_2) c_{13}(F_1, F_3) c_{14}(F_1, F_4) \\ \times c_{23|1}(F_{2|1}, F_{3|1}) c_{24|1}(F_{2|1}, F_{4|1}) \\ \times c_{34|12}(F_{3|12}, F_{4|12}) \end{cases} \quad (10)$$

Where the marginals are  $f_1 f_2 f_3 f_4$ ; the unconditional pairs are  $c_{12}(F_1, F_2)$ ,  $c_{13}(F_1, F_3)$ ,  $c_{14}(F_1, F_4)$ ; and the conditional pairs are  $c_{23|1}(F_{2|1}, F_{3|1})$ ,  $c_{24|1}(F_{2|1}, F_{4|1})$ , and  $c_{34|12}(F_{3|12}, F_{4|12})$ . The conditional distribution function  $F(x|v)$  for an  $n$ -dimensional vector  $v$  can be obtained using the h-function:

$$h(x|v, \theta) = F(x|v) = \frac{\partial C_{xv_j|v_{-j}}(F(x|v_{-j}), F(v_j|v_{-j}))}{\partial F(v_j|v_{-j})} \quad (11)$$

where  $v_j$  is an arbitrary component of  $v$ , and  $v_{-j}$  denotes the  $(n - 1)$ -dimensional vector  $v$  excluding  $v_j$ .

To fit the c-vine copula, the Dißmann algorithm (Dißmann et al. (2013) has been employed, which fits a vine copula by fitting the strongest dependencies first. This algorithm for C-vine copula is given as follows:

1. Calculate the empirical Kendall's tau  $\hat{\tau}_{j,k}$  for all possible variable pairs  $\{j, k\}$ ,  $1 \leq j < k \leq d$ .

2. Select the root node for C-vine:

Select the root node  $r$  that maximizes the sum of absolute empirical Kendall's taus:

$$r = \arg \max_{i=1,\dots,d} \sum_{k=1,k \neq i}^d |\hat{\tau}_{i,k}| \quad (12)$$

3. Construct Tree 1:

Set  $T_1 = \{\{r, k\} : k = 1, \dots, d, k \neq r\}$

4. For each edge  $\{r, k\}$  in  $T_1$ , select a copula and estimate the corresponding parameter(s). Then transform  $C_{r|k}(\mathbf{u}_r | \mathbf{u}_k)$  and  $C_{k|r}(\mathbf{u}_k | \mathbf{u}_r)$  using the fitted copula  $C_{rk}$ .

5. for  $i = 2, \dots, d - 1$  do {Iteration over the trees}

(a) Identify the new root node for Tree  $i$ :

The root of  $T_i$  is the edge in  $T_{i-1}$  that contains the root of  $T_{i-1}$ .

(b) Calculate the empirical Kendall's tau  $\hat{\tau}_{j,k|D}$  for all conditional variable pairs  $\{j, k|D\}$  where both edges contain the root of  $T_i$ .

(c) Construct Tree  $i$ :

Connect all edges that share the root node of  $T_i$ .

(d) For each edge  $\{j, k|D\}$  in  $T_i$ , select a conditional copula and estimate the corresponding parameter(s). Then transform  $C_{j|k \cup D}(\mathbf{u}_j | \mathbf{u}_k, \mathbf{u}_D)$  and  $C_{k|j \cup D}(\mathbf{u}_k | \mathbf{u}_j, \mathbf{u}_D)$  using the fitted copula  $C_{j,k|D}$ .

6. end for

After applying this algorithm, three matrices are obtained:  $M$  (Structure Matrix),  $P$  (Parameter Matrix), and  $C$  (Copula Type Matrix). The Structure Matrix  $M$  encodes the vine structure by specifying which variables are connected in each tree. The Parameter Matrix  $P$  contains the estimated parameters for each bivariate copula in the corresponding position. The Copula Type Matrix  $C$  identifies the type of copula selected for each edge according to the IDs. With these matrices and the desired number of samples  $n$ , we can generate random samples from the fitted C-vine copula using the following algorithm:

1. Flip the columns in the matrices vertically, such that the matrix becomes a lower triangular matrix.
2. Relabel the variables in  $M$ , such that the variables on the diagonal are ordered from  $d$  to 1, i.e.,  $m_{k,k} = d - k + 1$ ,  $k = 1, \dots, d$ .
3. Generate independent uniform samples  $U = [\mathbf{u}_1, \dots, \mathbf{u}_d]$  of length  $n$ , i.e.,  $\mathbf{u}_1 = [u_{11}, \dots, u_{n1}]$ .
4. Define  $V^{\text{direct}} = (v_{i,k}^{\text{direct}} | i, k = 1, \dots, d)$ .
5. Define  $V^{\text{indirect}} = (v_{i,k}^{\text{indirect}} | i, k = 1, \dots, d)$ .
6. Set  $[v_{d,1}^{\text{direct}}, v_{d,2}^{\text{direct}}, \dots, v_{d,d}^{\text{direct}}] = [\mathbf{u}_1, \mathbf{u}_2, \dots, \mathbf{u}_d]$ .
7. Let  $M = (\mathbf{m}_{i,k} | i, k = 1, \dots, d)$  with  $\mathbf{m}_{i,k} = \max\{m_{i,k}, \dots, m_{d,k}\}$  for all  $k = 1, \dots, d - 1$  and  $i = k, \dots, d$ .
8.  $\mathbf{x}_1 = v_{d,d}^{\text{direct}}$ .

9. for  $k = d - 1, \dots, 1$  do {Iterate over the columns of  $M$ }
  - (a) for  $i = k + 1, \dots, d$  do {Iterate over the rows of  $M$ }
  - i. if  $\mathbf{m}_{i,k} = m_{i,k}$ , then:
    - A. Set  $z_{i,k}^{(2)} = v_{i,(d-\mathbf{m}_{i,k}+1)}^{\text{direct}}$ .
    - ii. else:
      - A. Set  $z_{i,k}^{(2)} = v_{i,(d-\mathbf{m}_{i,k}+1)}^{\text{indirect}}$ .
      - iii. Set  $v_{d,k}^{\text{direct}} = h^{-1}(v_{d,k}^{\text{direct}}, z_{i,k}^{(2)} | t_{i,k}, p_{i,k})$ .
  - (b) end for
  - (c)  $\mathbf{x}_{d-k+1} = v_{d,k}^{\text{direct}}$ .
  - (d) for  $i = d, \dots, k + 1$  do {Iterate over the rows of  $M$ }
  - i. Set  $z_{i,k}^{(1)} = v_{i,k}^{\text{direct}}$ .
  - ii. Set  $v_{i-1,k}^{\text{direct}} = h(z_{i,k}^{(1)}, z_{i,k}^{(2)} | t_{i,k}, p_{i,k})$  and  $v_{i-1,k}^{\text{indirect}} = h(z_{i,k}^{(2)}, z_{i,k}^{(1)} | t_{i,k}, p_{i,k})$ .
- (e) end for
10. end for
  11. Sort the columns in  $X$  according to the sampling order, such that  $X$  is provided in the same order as the original data.

Where  $h()$  is the conditional CDF (h-function) and  $h^{-1}()$  is the inverse conditional CDF.

## 4.5 Risk Measurement and Model Evaluation

The performance of the EVT-Copula approach is evaluated against benchmark models using the original data obtained from the analysis. Value at Risk serves as the primary risk measure, with backtesting employed to assess forecast accuracy. Before calculating Value at Risk using the Monte Carlo simulation, the uniform samples generated from the fitted C-vine copula need to be transformed back to the original scale to obtain meaningful portfolio returns for risk assessment. This involves applying the inverse of the semi-parametric cumulative distribution function constructed earlier: for tail values, the inverse GPD transformation is applied, while for interior values, the inverse empirical distribution is used. This transformation ensures that the simulated standardized residuals maintain the distributional characteristics obtained from the GARCH filtering process while preserving the dependence structure obtained by the copula.

### 4.5.1 Value at Risk

Value at Risk (VaR) is defined as the maximum potential loss over a given time horizon at a specified confidence level. For a portfolio with return  $R_p$ , the VaR at confidence level  $\alpha$  is:

$$\text{VaR}_\alpha = -\inf\{r : P(R_p \leq r) \geq \alpha\} \quad (13)$$

where  $\alpha$  represent the confidence levels. In this paper, 95% and 99% are considered.

For the GARCH-EVT-Copula approach, the VaR calculation proceeds :

1. Generate  $N = 5,000$  samples from the fitted C-vine copula in the uniform domain  $[0, 1]^4$
2. Transform these uniform samples back to standardized residuals using the inverse semi-parametric CDF:
  - For values in the tail regions, apply the inverse GPD transformation
  - For values in the interior region, use the inverse empirical CDF
3. Convert standardized residuals  $z_{i,t+1}$  to returns using the GARCH model parameters:

$$r_{i,t+1} = \mu_i + \sigma_{i,t+1} \cdot z_{i,t+1} \quad (14)$$

where  $\sigma_{i,t+1}$  is the one-step-ahead volatility forecast from the GARCH model

4. Calculate portfolio returns assuming equal weights:

$$R_{p,t+1} = \frac{1}{4} \sum_{i=1}^4 r_{i,t+1} \quad (15)$$

5. Estimate VaR as the  $\alpha$ -quantile of the simulated portfolio return distribution

This procedure is performed throughout the out-of-sample period (January 2021 - December 2024), with model parameters re-estimated every trading days using a rolling window of 250 observations (approximately one year of trading days). The one-day-ahead VaR forecasts are then compared against realized portfolio returns for backtesting purposes.

### Kupiec POF Test (Unconditional Coverage)

The Kupiec (1995) test examines whether the observed frequency of VaR violations matches the expected frequency under the null hypothesis. Define the hit sequence as:

$$I_t = \begin{cases} 1 & \text{if } R_{p,t} < -\text{VaR}_{t|t-1}(\alpha) \\ 0 & \text{if } R_{p,t} \geq -\text{VaR}_{t|t-1}(\alpha) \end{cases} \quad (16)$$

where  $R_{p,t}$  is the realized portfolio return and  $\text{VaR}_{t|t-1}(\alpha)$  is the forecasted VaR. The proportion of violations is:

$$\hat{\pi} = \frac{1}{T} \sum_{t=1}^T I_t \quad (17)$$

Under the null hypothesis  $H_0 : \hat{\pi} = \alpha$ , the likelihood ratio test statistic is:

$$LR_{POF} = -2 \ln \left[ \frac{(1-\alpha)^{T-n} \alpha^n}{(1-\hat{\pi})^{T-n} \hat{\pi}^n} \right] \quad (18)$$

where  $n = \sum_{t=1}^T I_t$  is the number of violations. The test statistic follows a  $\chi^2(1)$  distribution asymptotically.

### Christoffersen Independence Test

While the Kupiec test evaluates the frequency of violations, it does not examine whether violations cluster over time. The Christoffersen (1998) test addresses this by testing whether violations are independently distributed.

The test constructs a first-order Markov chain with transition probabilities:

$$\pi_{ij} = P(I_t = j | I_{t-1} = i), \quad i, j \in \{0, 1\} \quad (19)$$

The empirical transition probabilities are estimated as:

$$\hat{\pi}_{ij} = \frac{n_{ij}}{n_{i0} + n_{i1}} \quad (20)$$

where  $n_{ij}$  is the number of transitions from state  $i$  to state  $j$ . The likelihood ratio test for independence is:

$$LR_{ind} = -2 \ln \left[ \frac{\hat{\pi}^{n_1} (1 - \hat{\pi})^{n_0}}{(\hat{\pi}_{01})^{n_{01}} (1 - \hat{\pi}_{01})^{n_{00}} (\hat{\pi}_{11})^{n_{11}} (1 - \hat{\pi}_{11})^{n_{10}}} \right] \quad (21)$$

where  $\hat{\pi} = (n_{01} + n_{11}) / (n_{00} + n_{01} + n_{10} + n_{11})$ . This statistic follows a  $\chi^2(1)$  distribution.

#### 4.5.2 Benchmark Model for Comparison

To evaluate the effectiveness of the GARCH-EVT-Copula approach, it is compared against the univariate GARCH model as a benchmark. This benchmark uses univariate GARCH models with Student-t distributed innovations for each asset, providing a baseline that captures volatility dynamics and fat tails but assumes no correlation or dependence between assets. By treating each asset independently, this model represents the simplest approach to portfolio VaR calculation, making it an ideal baseline for demonstrating the advantages of incorporating extreme value theory and copula-based dependencies.

The univariate GARCH-t VaR is calculated as follows: First, separate GARCH models with Student-t innovations are estimated for each asset's returns. Next, returns are simulated from each univariate model independently. These simulated returns are then combined using equal portfolio weights to obtain the portfolio return distribution. Finally, the VaR is estimated as the  $\alpha$ -quantile of this simulated portfolio return distribution. This approach captures volatility clustering and fat-tailed behavior in individual assets but fails to account for the co-movement patterns during extreme market events, which is precisely where the EVT-Copula framework aims to provide improvements.

## 5 Results

This section presents the empirical results following the methodology outlined in the previous section. The analysis proceeds through marginal model fitting, dependence structure estimation, and backtesting of the integrated GARCH-EVT-Copula approach against benchmark models.

### 5.1 Marginal Model Fitting Results

Using the processed data, the marginal distributions are first estimated through GARCH family models to capture the overall distribution dynamics, followed by EVT application to model the tail behavior more accurately.

#### 5.1.1 GARCH Family Model Estimation

Table 2: GARCH Family Models Estimation Results

Parameter	KOSPI (^KS11)			S&P 500 (^GSPC)			SSE (000001.SS)			Nikkei (^N225)		
	GARCH	GJR	EGARCH	GARCH	GJR	EGARCH	GARCH	GJR	EGARCH	GARCH	GJR	EGARCH
$\mu$	0.0495*** (0.0167)	0.0345** (0.0170)	0.0298 (0.0171)	0.0950*** (0.0138)	0.0739*** (0.0138)	0.0710*** (0.0138)	0.0388** (0.0191)	0.0389** (0.0193)	0.0398*** (0.0192)	0.0778*** (0.0220)	0.0454** (0.0214)	0.0403* (0.0214)
$\omega$	0.0394*** (0.0125)	0.0535*** (0.0162)	-0.0049 (0.0075)	0.0265*** (0.0075)	0.0303*** (0.0073)	-0.0038 (0.0073)	0.0138*** (0.0092)	0.0138*** (0.0051)	0.0163*** (0.0053)	0.0885** (0.0360)	0.1123*** (0.0291)	0.0274** (0.0112)
$\alpha$	0.1258*** (0.0233)	0.0408** (0.0175)	0.2135*** (0.0341)	0.2067*** (0.0309)	0.0564** (0.0226)	0.2518*** (0.0331)	0.0757*** (0.0125)	0.0761*** (0.0144)	0.1732*** (0.0241)	0.1441*** (0.0398)	0.0002 (0.0145)	0.2013*** (0.0432)
$\gamma$	- (0.0549)	0.1879*** (0.0255)	-0.1040*** (0.0604)	- (0.0206)	0.2848*** (0.0604)	-0.1685*** (0.0206)	- (0.0189)	-0.0009 (0.0163)	-0.0047 (0.0163)	- (0.0653)	0.3135*** (0.0299)	-0.1899*** (0.0299)
$\beta$	0.8363*** (0.0303)	0.8052*** (0.0368)	0.9500*** (0.0156)	0.7933*** (0.0261)	0.7906*** (0.0277)	0.9631*** (0.0086)	0.9206*** (0.0112)	0.9207*** (0.0116)	0.9885*** (0.0044)	0.8133*** (0.0519)	0.7841*** (0.0417)	0.9315*** (0.0206)
$\nu$	5.7081*** (0.7600)	5.9804*** (0.8370)	6.0074*** (0.8420)	4.7737*** (0.5230)	4.8917*** (0.5800)	4.9787*** (0.6200)	4.4631*** (0.4710)	4.4644*** (0.4730)	4.5152*** (0.4840)	4.8225*** (0.5260)	5.3365*** (0.6300)	5.4246*** (0.6460)
Log-Lik	-2359.45	-2343.74	-2342.91	-2297.50	-2276.97	-2274.63	-2779.70	-2779.69	-2776.21	-2918.85	-2882.02	-2876.30
AIC	4728.89	4699.48	4697.82	4604.99	4565.94	4561.25	5569.39	5571.39	5564.43	5847.70	5776.04	5764.60
BIC	4756.61	4732.74	4731.08	4632.71	4599.19	4594.51	5597.10	5604.64	5597.68	5875.42	5809.30	5797.86

Note: Standard errors in parentheses. \*, \*\*, \*\*\* denote significance at the 10%, 5%, and 1% levels, respectively. GJR denotes GJR-GARCH model. Log-lik denotes log-likelihood.

Table 2 presents the parameter estimates for all three GARCH specifications across the four markets. The results reveal several key findings that are crucial for understanding the tail behavior of our return distributions. First, all assets exhibit relatively low degrees of freedom, with  $\nu$  values ranging from 4 to 6. In the context of the Student's t-distribution, lower degrees of freedom imply heavier tails, indicating that extreme events are more likely than a normal distribution. The distribution only approaches normality as  $\nu \rightarrow \infty$ , and typically, when  $\nu > 30$ , the distribution can be considered approximately normal. The results, with all  $\nu$  values well below this threshold, confirm the presence of significant fat tail risk across all markets. Second, asymmetric effects are confirmed in both GJR-GARCH and EGARCH models. For the GJR-GARCH model, the positive and significant  $\gamma$  parameters indicate that negative shocks have a larger impact on future volatility than positive shocks of the same magnitude. This leverage effect is particularly pronounced in the S&P 500 ( $\gamma = 0.2848$ )

and Nikkei ( $\gamma = 0.3135$ ), while the SSE shows no significant asymmetry ( $\gamma = -0.0009$ , insignificant). The EGARCH model confirms these findings through negative  $\gamma$  parameters, with the S&P 500 ( $\gamma = -0.1685$ ) and Nikkei ( $\gamma = -0.1899$ ) again displaying the strongest asymmetric responses. Third, model selection criteria (AIC and BIC) provide additional insights into the relative performance of each specification. The EGARCH model consistently achieves the lowest AIC and BIC values across all four indices, indicating superior fit. This suggests that the EGARCH model provides the best overall fit for the data, confirming the presence of asymmetric volatility.

Given the significant findings from the GARCH models, particularly the presence of fat tails and asymmetric volatility, it is clear that while the Student's t-distribution captures the general fat tail behavior, it does not fully account for the extreme events that can occur in the tail. Extreme Value Theory (EVT) offers a more precise framework for modeling these extreme events, enabling a better understanding and quantification of the risks associated with such rare occurrences. Furthermore, due to the asymmetric volatility observed in the models, EVT should be applied separately to the upper and lower tails to accurately capture their distinct behaviors, rather than assuming symmetric tail behavior as traditional models do.

### 5.1.2 EVT

Table 3: EVT Model Results for GARCH-Filtered Residuals

Model	Index	Lower Tail (10%)			Upper Tail (10%)		
		$\xi$	$\sigma$	Threshold	$\xi$	$\sigma$	Threshold
EGARCH	KOSPI	-0.0487	0.7235	-1.2495	-0.0341	0.5195	1.1325
	S&P 500	0.1609	0.6969	-1.2216	-0.0516	0.4116	1.1047
	SSE	0.2099	0.5716	-1.1731	0.0725	0.5019	1.1076
	Nikkei	0.0436	0.6587	-1.2068	0.0190	0.5095	1.1536
GARCH	KOSPI	-0.0349	0.7185	-1.2947	-0.1345	0.5418	1.1010
	S&P 500	0.0958	0.7431	-1.2559	-0.0682	0.4155	1.0796
	SSE	0.1170	0.6540	-1.1536	0.0342	0.5477	1.0859
	Nikkei	-0.0004	0.6998	-1.2509	-0.0432	0.5126	1.1314
GJR-GARCH	KOSPI	-0.0730	0.7449	-1.2483	-0.0362	0.5283	1.1204
	S&P 500	0.1635	0.6837	-1.2330	-0.0156	0.3949	1.1076
	SSE	0.1195	0.6513	-1.1550	0.0349	0.5462	1.0867
	Nikkei	0.0711	0.6331	-1.2278	-0.0275	0.5372	1.1391

Note:  $\xi$  denotes the shape parameter and  $\sigma$  denotes the scale parameter of the Generalized Pareto Distribution (GPD). Negative  $\xi$  indicates a thin tail (finite endpoint), while positive  $\xi$  indicates a heavy tail. All models use 10% tail fractions with 189 observations in each tail.

Table 3 presents the EVT estimation results across different GARCH models using standardized residuals. Based on the shape parameter, most data exhibit heavy tails in the lower tail across all models, except for KOSPI. KOSPI also shows a thin tail in the upper tail, suggesting that the market does not experience significant extreme events, unlike the other markets. For S&P 500 and Nikkei (excluding the Nikkei EGARCH model), a thin upper tail is observed, indicating larger downside risks. This reflects the leverage effect, where negative shocks tend to impact future volatility more than positive shocks of the same magnitude. In contrast, for SSE, heavy tails are observed in both the upper and lower tails, suggesting a higher frequency of extreme events in both directions. This indicates that the SSE market is more vulnerable to extreme fluctuations in both upward and downward directions.

The consistency of these patterns across GARCH, GJR-GARCH, and EGARCH models highlights the robustness of our EVT results. Regardless of the volatility filtering method used, the fundamental tail characteristics remain stable, reinforcing the reliability of the extreme value analysis. Furthermore, the threshold values reveal interesting asymmetry: lower tail thresholds consistently show larger absolute values than upper tail thresholds (ranging from -1.15 to -1.29 versus 1.08 to 1.15). This asymmetry reflects the negative skewness in the return distributions, further validating that the EVT framework captures the tail behavior of these stock datasets.

### Semi-parametric CDFs with GPD Tails (GJR-GARCH Model)

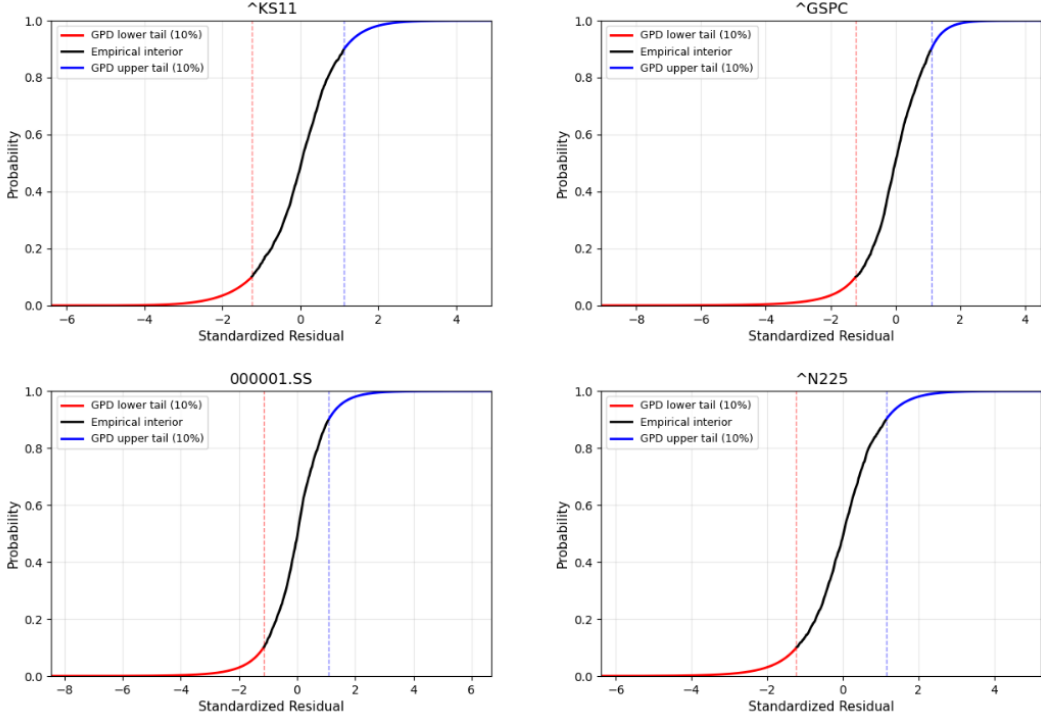


Figure 3: Semi-parametric CDFs with GPD Tails (GJR-GARCH Model)

Note : Empirical distributions (black) combined with GPD fits for lower (red) and upper (blue) tails at 10% thresholds (vertical dashed lines) for GJR-GARCH filtered residuals.

Figure 3 displays the semi-parametric cumulative distribution functions (CDFs) with GPD tails estimated from the GJR-GARCH model. Consistent with the earlier analysis, KOSPI exhibits steep slopes in both lower and upper tails, confirming the presence of thin tails, where the probability of extreme events diminishes rapidly. The S&P 500 demonstrates a more gradual slope in the lower tail compared to the upper tail, indicating a heavier lower tail. The SSE, as suggested by the EVT results, shows relatively gradual slopes in both tails, though the lower tail extends further. Nikkei also displays a longer lower tail relative to its upper tail. Notably, across all markets, the lower tail spans a wider range on the horizontal axis than the upper tail, which is relatively narrow. This asymmetry provides visual confirmation that downside risks are more extreme than upside risk across all four markets. The corresponding semi-parametric CDFs for GARCH and EGARCH models are provided in B.1 for comparison. Additionally, goodness-of-fit tests were employed to validate the GPD specifications. Both the Cramér-von Mises and Anderson-Darling tests indicate that all assets, except for EGARCH model for S&P 500 lower tail in the Cramér-von Mises test, pass the goodness-of-fit criteria across all GARCH model specifications at the 5% significance level. Detailed test statistics and p-values are provided in the Appendix.

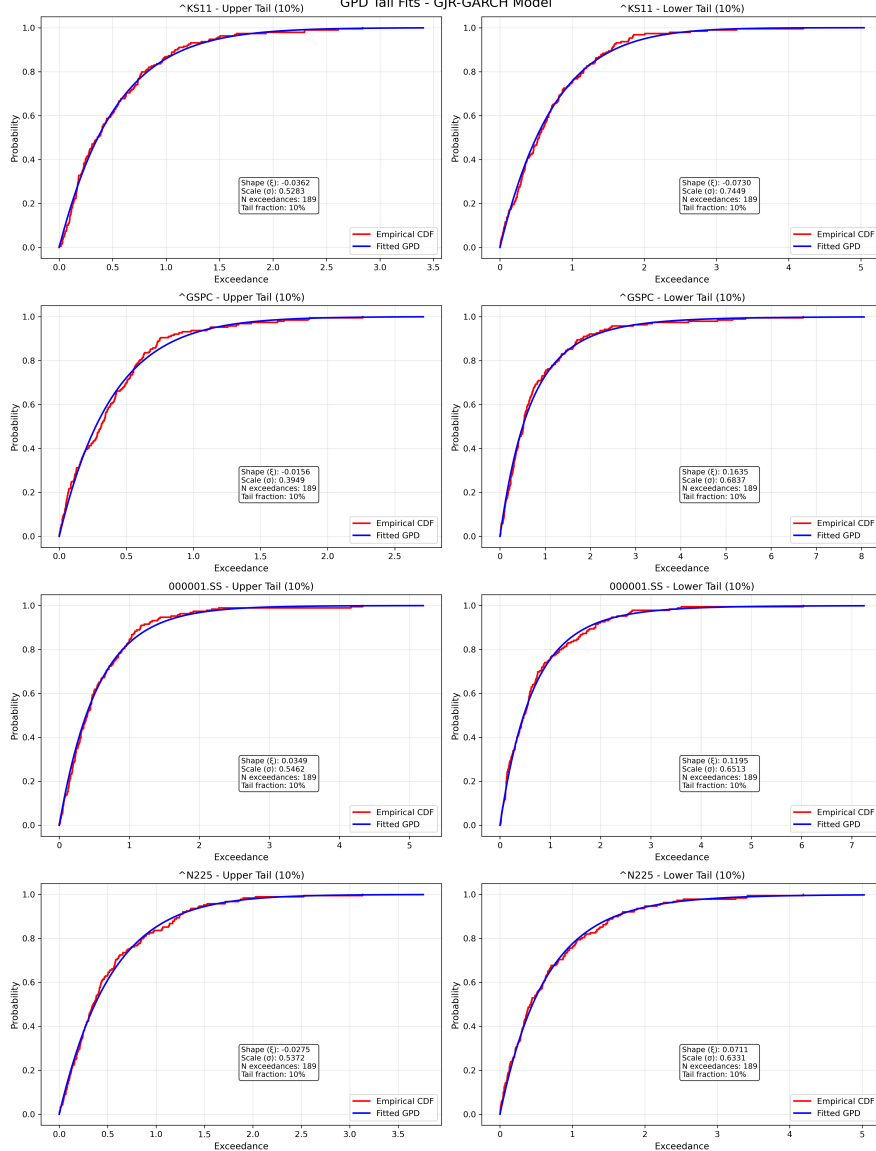


Figure 4: GPD Tail Fits for GJR-GARCH Model

Note: Empirical CDFs (red) versus fitted GPD CDFs (blue) for exceedances in upper and lower 10% tails across four market indices. The close fit validates the GPD specification for extreme value modeling.

Figure 4 presents the GPD tail fits for the GJR-GARCH model, providing visual validation of the GPD specification for both lower and upper tails. The empirical cumulative distribution functions (red lines) and the fitted GPD models (blue lines) demonstrate strong agreement across all assets and tails. This close correspondence between the empirical and theoretical distributions indicates that the GPD adequately captures the extreme value behavior, corroborating the goodness-of-fit test results presented earlier. The corresponding tail fit plots for the GARCH and EGARCH models, which exhibit similar patterns, are provided in B.3.

## 5.2 Copula Fitting Results

Building on the marginal distribution estimates from the previous section, the joint dependence structure between markets is examined using C-vine copulas. This approach explores the interaction between market pairs, conditional on KOSPI, and highlights how their co-movements behave, particularly focused on tail dependence. The following presents the C-vine copula estimation results, focusing on the dependence structure across the four markets under different models.

Table 4: C-Vine Copula Estimation Results Centered at KOSPI

Model	Copula Pair	Tree 1		Tree 2		Tree 3
		Type	Parameter(s)	Type	Parameter	Type & Parameter
EGARCH	(KOSPI, S&P 500)	Gumbel180	1.1334	—	—	—
	(KOSPI, SSE)	Gumbel180	1.2551	—	—	—
	(KOSPI, Nikkei)	Student	$\rho = 0.5479$	$\nu = 7.3148$	—	—
	(S&P 500, Nikkei KOSPI)	—	—	Gumbel180	1.0536	—
	(SSE, Nikkei KOSPI)	—	—	Gaussian	0.1244	—
	(S&P 500, SSE Nikkei, KOSPI)	—	—	—	—	Frank: 0.2648
GARCH	(KOSPI, S&P 500)	Gumbel180	1.1344	—	—	—
	(KOSPI, SSE)	Gumbel180	1.2600	—	—	—
	(KOSPI, Nikkei)	Gumbel180	1.5790	—	—	—
	(S&P 500, Nikkei KOSPI)	—	—	Gumbel180	1.0576	—
	(SSE, Nikkei KOSPI)	—	—	Gaussian	0.1243	—
	(S&P 500, SSE Nikkei, KOSPI)	—	—	—	—	Frank: 0.2351
GJR-GARCH	(KOSPI, S&P 500)	Gumbel180	1.1307	—	—	—
	(KOSPI, SSE)	Gumbel180	1.2565	—	—	—
	(KOSPI, Nikkei)	Student	$\rho = 0.5469$	$\nu = 7.5311$	—	—
	(S&P 500, Nikkei KOSPI)	—	—	Gumbel180	1.0531	—
	(SSE, Nikkei KOSPI)	—	—	Gaussian	0.1225	—
	(S&P 500, SSE Nikkei, KOSPI)	—	—	—	—	Frank: 0.2478

Note: The table presents C-Vine copula structures estimated for standardized residuals from three GARCH models with KOSPI as the center asset. Gumbel180 indicates a rotated Gumbel copula capturing lower tail dependence. Student copula parameters include correlation ( $\rho$ ) and degrees of freedom ( $\nu$ ). All models use 10% tail fractions for EVT modeling with 1,887 observations.

Table 4 presents the C-vine copula estimation results centered at KOSPI. First, the difference in the copula results across the different models was not significant. Only in Tree 1 did the GARCH model estimate a Gumbel copula for (KOSPI, Nikkei), while the other models estimated a Student copula. This suggests that the dependence structure remains stable regardless of the different volatility filtering methods.

At Tree 1, for both pairs, (S&P 500, KOSPI) and (SSE, KOSPI), the Gumbel 180 copula is selected, indicating that these pairs exhibit lower tail dependence. This suggests that in extreme negative market movements, the S&P 500 and SSE markets tend to move in the same direction as KOSPI, as the Gumbel copula captures the stronger co-movements of the markets during downward market shocks. The Student copula is selected for the (KOSPI, Nikkei) pair, indicating that the relationship between KOSPI and Nikkei is best modeled by tail dependence combined with correlation. The parameters of this copula, including correlation ( $\rho = 0.5479$ ) and degrees of freedom ( $\nu = 7.3148$ ), indicate that KOSPI and Nikkei are moderately correlated during extreme market events, with a non-normal joint tail structure.

At Tree 2, for the pair (S&P 500, Nikkei — KOSPI), the Gumbel180 copula is used conditionally on KOSPI, which is particularly suited for modeling lower tail dependence and capturing extreme co-movements during downward market shocks. This suggests that even when KOSPI is considered as a conditioning factor, the extreme co-movement between S&P 500 and Nikkei remains dominant during negative shocks, with both assets tending to move in the same direction during severe market downturns. In contrast, for the pair (SSE, Nikkei — KOSPI), the Gaussian copula is estimated, indicating a weaker and more stable linear relationship between SSE and Nikkei, even when conditioned on KOSPI. This suggests that their correlation is relatively weak, particularly during extreme market events where joint tail behavior is less pronounced compared to other asset pairs.

At Tree 3, for the pair (S&P 500, SSE — Nikkei, KOSPI), the Frank copula is estimated. The Frank copula is known for modeling symmetric dependence structures, which implies that the relationship between S&P 500 and SSE remains relatively stable even when conditioned on KOSPI and Nikkei. In other words, despite the conditioning on KOSPI and Nikkei, the dependence between S&P 500 and SSE does not change significantly. The estimated parameter of 0.2648 is relatively low, suggesting that the dependence between these two assets, when conditioned on KOSPI and Nikkei, is weak but stable.

Table 5: Tail Dependence Coefficients for C-Vine Copula Models

Model	Copula Pair	Tree	Copula Type	$\lambda_L$	$\lambda_U$
EGARCH	KOSPI-S&P 500	1	Gumbel180	0.155	0
	KOSPI-SSE	1	Gumbel180	0.212	0
	KOSPI-Nikkei	1	Student	0.189	0.189
	S&P 500-Nikkei KOSPI	2	Gumbel180	0.063	0
	SSE-Nikkei KOSPI	2	Gaussian	0	0
	S&P 500-SSE Nikkei,KOSPI	3	Frank	0	0
GARCH	KOSPI-S&P 500	1	Gumbel180	0.156	0
	KOSPI-SSE	1	Gumbel180	0.214	0
	KOSPI-Nikkei	1	Gumbel180	0.319	0
	S&P 500-Nikkei KOSPI	2	Gumbel180	0.070	0
	SSE-Nikkei KOSPI	2	Gaussian	0	0
	S&P 500-SSE Nikkei,KOSPI	3	Frank	0	0
GJR-GARCH	KOSPI-S&P 500	1	Gumbel180	0.153	0
	KOSPI-SSE	1	Gumbel180	0.213	0
	KOSPI-Nikkei	1	Student	0.185	0.185
	S&P 500-Nikkei KOSPI	2	Gumbel180	0.063	0
	SSE-Nikkei KOSPI	2	Gaussian	0	0
	S&P 500-SSE Nikkei,KOSPI	3	Frank	0	0

Note:  $\lambda_L$  and  $\lambda_U$  denote lower and upper tail dependence coefficients. For Gumbel180:  $\lambda_L = 2 - 2^{1/\theta}$ . For Student:  $\lambda_L = \lambda_U = 2t_{\nu+1}(-\sqrt{(\nu+1)(1-\rho)/(1+\rho)})$ . Gaussian and Frank copulas have zero tail dependence.

The tail dependence coefficients provide crucial insights into extreme co-movements among East Asian markets. When KOSPI is paired with other assets, the predominance of Gumbel180 copulas reveals strong asymmetric dependence, with lower tail coefficients ranging from 0.15 to 0.32 but zero upper tail dependence, confirming that these markets crash together but do not increase together—a phenomenon particularly pronounced in the KOSPI-Nikkei pair under GARCH ( $\lambda_L = 0.319$ ). Interestingly, under EGARCH and GJR-GARCH models, the KOSPI-Nikkei pair follows a Student copula with symmetric tail dependence ( $\lambda_L = \lambda_U \approx 0.19$ ), indicating that these two markets exhibit extreme co-movements in both positive and negative extreme events, reflecting their deep economic integration and similar market structures.

The hierarchical structure of the C-vine reveals that while direct KOSPI link show substantial tail dependence (Tree 1:  $\lambda_L = 0.15\text{--}0.32$ ), the conditional dependencies are much weaker: S&P 500-Nikkei given KOSPI shows minimal tail dependence ( $\lambda_L = 0.06\text{--}0.07$ ), and SSE-Nikkei given KOSPI exhibits zero tail dependence. To further investigate these relationships, D-vine structures, which allow for direct pairwise connections, were also estimated. The D-vine results (presented in C.1) reveal that S&P 500 and Nikkei indeed exhibit moderate direct tail dependence ( $\lambda_L \approx 0.14$ ) when paired unconditionally, while S&P 500-SSE shows no tail dependence even in direct pairing. This suggests that while a US-Japan financial channel exists independently of KOSPI, the dramatic reduction in conditional dependencies in the C-vine structure confirms that KOSPI captures a significant portion of the regional contagion dynamics.

### 5.3 VaR Backtesting Results

To evaluate the effectiveness of the EVT-Copula approach in capturing portfolio tail risk, a backtesting analysis was conducted, comparing the EVT-Copula models against the traditional GARCH-t model as a benchmark. Table 6 summarizes the out-of-sample performance of four models: the benchmark GARCH-t model and three EVT-Copula variants (EGARCH, GARCH, and GJR-GARCH), all of which incorporate tail dependence using C-vine copulas. The results highlight key differences in model performance. The GARCH-t benchmark model assumes that asset returns follow a univariate Student-t distribution for modeling volatility, but it assumes no correlation between the assets. It was observed that the performance of this model is notably inadequate. Both the coverage and independence tests are rejected at the 1% significance level across all VaR levels (95% and 99%). This indicates that the

Table 6: Portfolio VaR Backtesting Results

Model	VaR Level	Violations			Kupiec Test		Independence Test	
		Count	Rate	Expected	LR Stat	p-value	Ind Stat	p-value
GARCH-t	95%	33	6.82%	5.00%	6.425	0.011*	11.597	0.001***
	99%	16	3.31%	1.00%	16.525	0.000***	6.309	0.012*
EGARCH-EVT-Copula	95%	20	4.13%	5.00%	2.865	0.091	1.333	0.248
	99%	9	1.86%	1.00%	3.063	0.080	2.070	0.150
GARCH-EVT-Copula	95%	18	3.72%	5.00%	3.675	0.055	4.997	0.025*
	99%	8	1.65%	1.00%	1.902	0.168	2.508	0.113
GJR-GARCH-EVT-Copula	95%	18	3.72%	5.00%	3.675	0.055	4.997	0.025*
	99%	7	1.45%	1.00%	0.996	0.318	3.026	0.082

Notes: Backtesting results for 484 out-of-sample observations with 250-day rolling windows and equal weights. \*, \*\*, \*\*\* denote significance at 10%, 5%, and 1% levels.

GARCH-t model fails to capture the true tail risk behavior of the portfolio, especially in terms of the extreme risk events that often occur in financial markets.

In contrast, the EVT-Copula models, which explicitly account for tail dependencies between assets, demonstrate significantly improved performance. The optimal model varies depending on the confidence level. For the 95% VaR level, the EGARCH-EVT-Copula model performs best with a violation rate of 4.13%, which is closest to the expected 5.00%. It passes both the Kupiec test (p-value: 0.091) and the independence test (p-value: 0.248), indicating that it effectively captures both the frequency and clustering patterns of extreme events at this confidence level. For the 99% VaR level, the GJR-GARCH-EVT-Copula model performs best. With a violation rate of 1.45% (compared to the expected 1.00%), it maintains acceptable accuracy while passing both statistical tests with comfortable margins (Kupiec p-value: 0.318, independence p-value: 0.082). This suggests that the GJR-GARCH specification, which captures leverage effects in volatility, is particularly effective for modeling more extreme tail events.

These findings underline the ability of the EVT-Copula models to better capture extreme tail behavior in financial portfolios. By incorporating both the EVT for tail modeling and the copula for capturing asymmetric dependencies, these models offer a more comprehensive and accurate risk assessment.

## 6 Conclusion

This paper examined tail risk dependencies in East Asian financial markets using a GARCH-EVT-Copula framework, focusing on the Korean market. Several important findings emerge. First, all markets exhibit fat tails, with downside risks more pronounced than upside risks, indicating asymmetric tail behavior. Second, copula analysis shows that KOSPI has lower tail dependence with the S&P 500 and SSE, while the KOSPI-Nikkei pair exhibits symmetric tail dependence under EGARCH and GJR-GARCH models but lower tail dependence under the GARCH model. Third, the EVT-Copula approach demonstrates superior Value-at-Risk forecasting performance compared to the GARCH-t benchmark, with the EGARCH-EVT-Copula model performing best at the 95% level and the GJR-GARCH-EVT-Copula model at the 99% level. These results indicate that East Asian markets tend to move together during crises, underscoring the importance of modeling tail dependencies for effective risk management.

However, this study has limitations. The analysis employed a fixed 10% quantile threshold for EVT without conducting sensitivity analysis, which may affect the accuracy of tail estimates under different market conditions. Additionally, the scope of the dataset was limited to the KOSPI alongside three major indices, which, while capturing key regional dynamics, may not fully reflect broader market interactions within East Asia. The study also relied on the GARCH family as the volatility filter, leaving potential improvements unexplored through alternative methods such as DCC-GARCH, realized volatility models, or stochastic volatility models with heavy-tailed distributions. Future research could extend this framework by applying these alternative models, incorporating a wider set of regional and global indices, and testing different EVT thresholds to assess the robustness of tail risk estimates.

## A Stochastic Volatility with Normal Distribution

Although the GARCH model was the main model used in this paper, the Stochastic Volatility (SV) model also offers valuable insights. The SV model allows for the dynamic estimation of volatility, which is crucial for risk analysis. However, estimating the SV model is not straightforward, especially when using distributions like the Student t-distribution, which can be challenging to estimate. Therefore, in this paper, a normal distribution is chosen for simplicity. The estimation is employed using the Quasi-Maximum Likelihood (QML) method, proposed by [Harvey et al. \(1994\)](#). By linearizing the model through log-squared returns and applying the Kalman filter, QML offers a computationally efficient alternative to more complex methods like MCMC or simulated maximum likelihood, while still capturing the essential volatility dynamics needed for our tail risk analysis.

### A.1 Methodology

The stochastic volatility model for the daily log return is defined as follows:

$$y_t = \mu + \sigma \exp\left(\frac{\alpha_t}{2}\right) \epsilon_t, \quad \epsilon_t \sim N(0, 1)$$

$$\alpha_{t+1} = \phi \alpha_t + \eta_t, \quad \eta_t \sim N(0, \sigma_\eta^2)$$

with  $\sigma, \sigma_\eta > 0$  and  $0 < \phi < 1$ .

The observations are then transformed to obtain a linear model, so that the Kalman filter can be applied as follows:

$$x_t := \log(y_t - \mu)^2 = \log(\sigma^2) + \alpha_t + \log(\epsilon_t^2).$$

The above observation equation is linear in the state,  $\alpha_t$ , but the disturbance term,  $\log(\epsilon_t^2)$ , is non-Gaussian. In particular, when assuming  $\epsilon_t \sim N(0, 1)$  as in (1),  $\log(\epsilon_t^2)$  follows the  $\log \chi^2$  distribution, which has mean  $E[\log(\epsilon_t^2)] = -1.27$  and variance  $\text{Var}[\log(\epsilon_t^2)] = \pi^2/2 = 4.93$ . However, to use the Kalman filter, the disturbance terms must have mean zero. Define the transformed disturbance term  $\xi_t := \log(\epsilon_t^2) + 1.27$  and intercept term  $\kappa := \log(\sigma^2) - 1.27$ . By assuming that the transformed disturbance terms are Gaussian,  $\xi_t \sim N(0, 4.93)$ , the following approximate state space model is obtained:

$$x_t = \kappa + \alpha_t + \xi_t, \quad \xi_t \sim N(0, 4.93),$$

$$\alpha_{t+1} = \phi \alpha_t + \eta_t, \quad \eta_t \sim N(0, \sigma_\eta^2),$$

with parameter vector  $\psi = (\kappa, \phi, \sigma_\eta^2)'$ . As the above model is linear Gaussian, the Kalman filter can be used for approximate analysis and parameter estimation. To estimate the parameters of the SV model, a log-likelihood function is defined based on the Kalman filter's predictions and updates. The log-likelihood is calculated by comparing the predicted values with the observed values and considering the innovation (the difference between the transformed data and the predicted state). The function is then maximized to estimate the model parameters. This step ensures that the model parameters are chosen to best fit the observed data. Once the log-likelihood function is defined, an optimization procedure is used to find the optimal parameters. In this case, the Quasi-Maximum Likelihood (QML) method is used, where the parameters are estimated by minimizing the negative log-likelihood. This optimization is performed using numerical techniques such as L-BFGS-B, which is a quasi-Newton method commonly used for large-scale optimization problems. By iterating over different parameter values, the method converges to the set of parameters that maximizes the likelihood function.

## A.2 Result

Table 7: Stochastic Volatility Model Estimation Results

Index	Parameter Estimates					
	$\kappa$	$\phi$	$\sigma_\eta^2$	$\sigma$	Log-Lik	$\sigma$
KOSPI	-1.867	0.962	0.0534	0.7420	-4376.88	0.7420
S&P 500	-1.910	0.967	0.0934	0.7263	-4326.78	0.7263
SSE	-1.467	0.989	0.0185	0.9062	-4338.70	0.9062
Nikkei	-1.265	0.950	0.0726	1.0025	-4309.35	1.0025

Note: Quasi-Maximum Likelihood (QML) estimates for the SV model:  $x_t = \kappa + \alpha_t + \xi_t$  where  $\alpha_{t+1} = \phi\alpha_t + \sigma_\eta\eta_t$ . The volatility scale parameter is calculated as  $\sigma = \exp((\kappa + 1.27)/2)$ .

Table 8: EVT Model Parameters for Stochastic Volatility-Filtered Residuals

Market	Lower Tail (10%)			Upper Tail (10%)		
	Shape ( $\xi$ )	Scale ( $\sigma$ )	Threshold	Shape ( $\xi$ )	Scale ( $\sigma$ )	Threshold
KOSPI	0.3010	0.6684	-2.0279	0.2025	0.3527	0.2724
S&P 500	0.3114	0.9432	-2.2173	0.2088	0.3090	0.2600
SSE	0.3333	1.0988	-2.5032	0.0298	0.6942	0.2872
Nikkei	-0.0212	1.1602	-2.7193	0.1135	0.6062	0.3590

Notes: The table presents the Generalized Pareto Distribution (GPD) parameters estimated for the 10% tails of stochastic volatility-filtered residuals. Shape parameter  $\xi$  indicates tail heaviness, scale parameter  $\sigma$  measures dispersion, and threshold values determine the cutoff points for extreme value modeling.

Table 7 presents the SV model estimation results across the four markets. The persistence parameters ( $\phi$ ) range from 0.950 to 0.989, indicating high volatility persistence across all markets.

More importantly, Table 8 reveals notable differences in tail behavior when using SV-filtered residuals compared to GARCH-filtered residuals. First, all markets except Nikkei exhibit heavy tails in the lower tail (positive  $\xi$  values), with shape parameters ranging from 0.3010 to 0.3333, indicating substantially heavier tails than those observed in the GARCH models. This asymmetry clearly demonstrates that downside risks are more pronounced than upside risks across East Asian markets.

Second, the threshold values for the lower tails are considerably more extreme than those from GARCH models, ranging from -2.0279 (KOSPI) to -2.7193 (Nikkei), compared to the typical range of -1.15 to -1.29 in GARCH models. This substantial difference suggests that the SV model captures more extreme volatility dynamics. These findings underscore the importance of volatility model specification in tail risk assessment, as different volatility filters can lead to notably different conclusions.

Figure 5 visualizes the semi-parametric CDFs with GPD tails for SV model residuals. The plots reveal dramatically extended lower tails compared to the GARCH models, with the horizontal axis extending from approximately -12.5 to 5 for most markets. This wide range, particularly in the negative direction, confirms the presence of severe downside tail risk. Notably, the upper tails (blue lines) are relatively narrow, further emphasizing the asymmetric tail in these markets under the SV framework.

### Semi-parametric CDFs with GPD Tails (Stochastic Volatility Model)

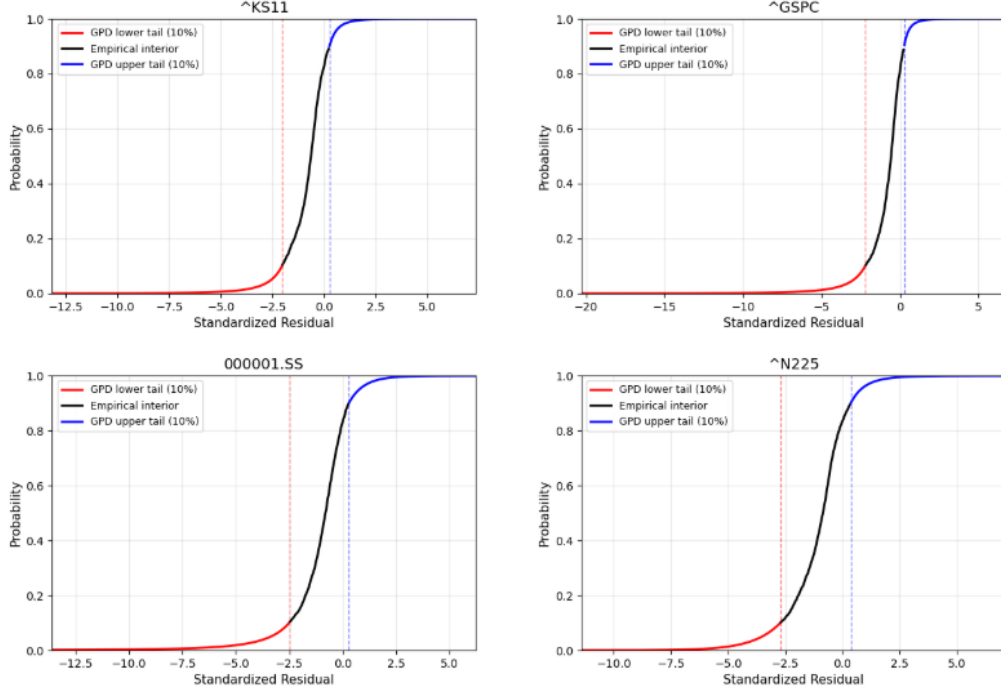


Figure 5: Semi-parametric CDFs with GPD Tails (SV Model)

Note: Empirical distributions (black) combined with GPD fits for lower (red) and upper (blue) tails at 10% thresholds (vertical dashed lines) for SV-filtered residuals.

Table 9: C-Vine Copula Structure for SV-EVT Model

Tree	Edge	Copula Type	Parameter 1	Parameter 2	$\lambda_L$	$\lambda_U$
1	S&P 500-KOSPI	Student-t	0.256	4.222	0.094	0.094
	SSE-KOSPI	Gumbel180	1.265	—	0.185	0.000
	KOSPI-Nikkei	Student-t	0.562	6.779	0.314	0.314
2	S&P 500-Nikkei KOSPI	Student-t	0.124	7.423	0.023	0.023
	SSE-Nikkei KOSPI	Gumbel180	1.077	—	0.073	0.000
3	S&P 500-SSE Nikkei,KOSPI	Frank	0.494	—	0.000	0.000

Notes: The table presents the estimated C-vine copula structure for the SV-EVT model using 1,887 observations with KOSPI as the central node.  $\lambda_L$  and  $\lambda_U$  denote lower and upper tail dependence coefficients, respectively. For Student-t copula:  $\lambda = 2t_{df+1}(-\sqrt{(df+1)(1-\rho)/(1+\rho)})$ . For Gumbel180:  $\lambda_L = 2 - 2^{1/\alpha}$ ,  $\lambda_U = 0$ . For Frank copula:  $\lambda_L = \lambda_U = 0$ .

Table 9 shows the results of the C-vine copula structure. A notable difference from the GARCH models is that the relationship between S&P 500 and KOSPI is now captured by a Student-t copula, indicating symmetric tail dependence ( $\lambda_L = \lambda_U = 0.094$ ) rather than the asymmetric Gumbel180 copula found in GARCH specifications. This suggests that under the SV framework, extreme co-movements between the US and Korean markets occur in both directions. In Tree 2, the conditional relationships also show different copula selections. The S&P 500-Nikkei pair conditioned on KOSPI is modeled by a Student-t copula with very low symmetric tail dependence ( $\lambda_L = \lambda_U = 0.023$ ), while the SSE-Nikkei pair conditioned on KOSPI maintains the Gumbel180 copula with lower tail dependence only ( $\lambda_L = 0.073$ ). Tree 3 shows consistent results with the GARCH models, where the S&P 500-SSE relationship conditioned on both Nikkei and KOSPI is captured by a Frank copula, indicating no tail dependence. Among all assets connected to KOSPI, the Nikkei exhibits the highest tail dependence ( $\lambda_L = \lambda_U = 0.314$ ), which is consistent with the findings from the GARCH models. This reinforces

the strong integration between the Korean and Japanese markets during extreme events, regardless of the volatility specification used.

Table 10: VaR Backtesting Results for SV-EVT-Copula Model

VaR Level	Violations		Kupiec Test		Independence Test	
	Count	Rate	LR Stat	p-value	Ind Stat	p-value
95%	17	3.51%	4.249	0.039*	2.275	0.132
99%	6	1.24%	0.382	0.537	3.649	0.056

Notes: Backtesting results for 484 out-of-sample observations. Expected violation rates are 5.00% and 1.00% for 95% and 99% VaR levels, respectively. \*, \*\*, \*\*\* denote significance at 10%, 5%, and 1% levels.

Table 10 exhibits the backtesting results for the SV-EVT-Copula model. Except for the Kupiec test at the 95% level, which rejects the null hypothesis with a p-value of 0.039, the model demonstrates good performance. Notably, at the 99% confidence level, the SV-EVT-Copula model shows excellent results with both the Kupiec test (p-value = 0.537) and the independence test (p-value = 0.056) failing to reject their respective null hypotheses. This indicates that the model accurately captures extreme tail risks at the 99% level.

Remarkably, despite the simplifying assumption of normality in the SV specification, the model achieves competitive performance. This suggests that the stochastic volatility framework, combined with EVT and copula modeling, provides an alternative approach for characterizing extreme market risks. However, given the heavy-tailed nature of financial returns observed throughout this study, future research should consider implementing the SV model with a Student-t distribution assumption, which may further improve the model's ability to capture extreme events and provide more accurate tail risk measurements.

## B Extreme Value Theory

### B.1 Semi-parametric CDFs Plot

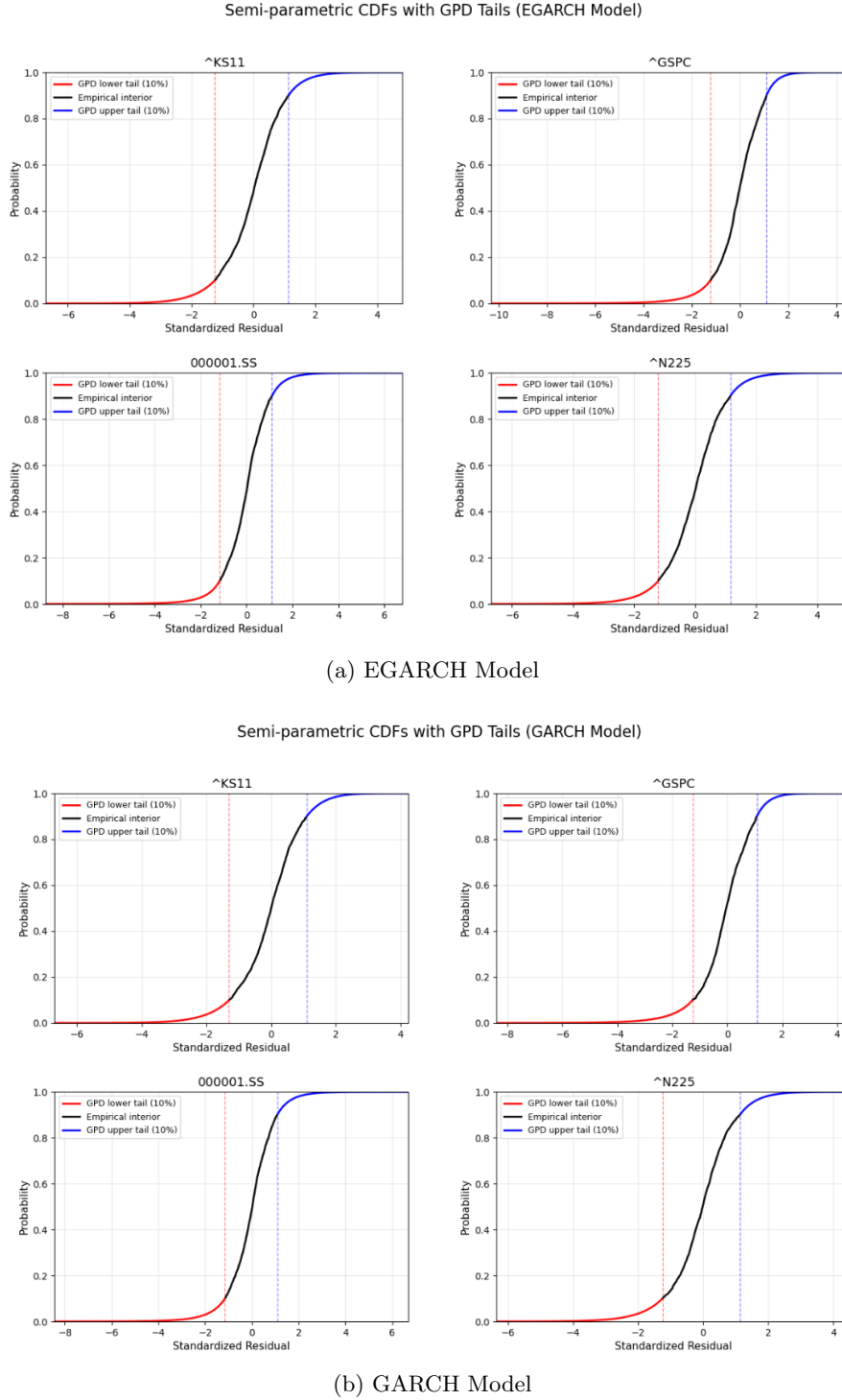


Figure 6: Semi-parametric CDFs with GPD Tails

Note : Empirical distributions (black) combined with GPD fits for lower (red) and upper (blue) tails at 10% thresholds (vertical dashed lines) for EGARCH and GARCH filtered residuals.

## B.2 GPD Goodness-of-Fit

Table 11: GPD Goodness-of-Fit Test Results for GARCH Family Models

Asset	Model	Tail	n	GPD Parameters		Cramér-von Mises		Anderson-Darling	
				Shape ( $\xi$ )	Scale ( $\sigma$ )	$W^2$	p-value	$A^2$	p-value
KOSPI	EGARCH	Lower	189	-0.0487	0.7235	0.0435	0.690	0.3080	0.714
		Upper	189	-0.0341	0.5195	0.0485	0.606	0.2775	0.752
	GARCH	Lower	189	-0.0349	0.7185	0.0293	0.870	0.1964	0.930
		Upper	189	-0.1345	0.5418	0.0613	0.444	0.3343	0.622
	GJR-GARCH	Lower	189	-0.0730	0.7449	0.0610	0.448	0.4369	0.410
		Upper	189	-0.0362	0.5283	0.0677	0.370	0.6380	0.178
S&P 500	EGARCH	Lower	189	0.1609	0.6969	0.1517	0.042*	0.8586	0.076
		Upper	189	-0.0516	0.4116	0.1031	0.164	0.5864	0.260
	GARCH	Lower	189	0.0958	0.7431	0.0880	0.212	0.6052	0.188
		Upper	189	-0.0682	0.4155	0.0460	0.652	0.3605	0.590
	GJR-GARCH	Lower	189	0.1635	0.6837	0.0925	0.170	0.5517	0.220
		Upper	189	-0.0156	0.3949	0.1387	0.054	0.8361	0.080
SSE	EGARCH	Lower	189	0.2099	0.5716	0.0810	0.238	0.7391	0.102
		Upper	189	0.0725	0.5019	0.0598	0.456	0.4422	0.426
	GARCH	Lower	189	0.1170	0.6540	0.0576	0.414	0.4097	0.416
		Upper	189	0.0342	0.5477	0.0909	0.238	0.6257	0.198
	GJR-GARCH	Lower	189	0.1195	0.6513	0.0572	0.456	0.4012	0.448
		Upper	189	0.0349	0.5462	0.0883	0.196	0.6079	0.190
Nikkei	EGARCH	Lower	189	0.0436	0.6587	0.0208	0.968	0.2143	0.904
		Upper	189	0.0190	0.5095	0.1135	0.110	0.6282	0.192
	GARCH	Lower	189	-0.0004	0.6998	0.0913	0.224	0.5941	0.242
		Upper	189	-0.0432	0.5126	0.0803	0.284	0.6103	0.232
	GJR-GARCH	Lower	189	0.0711	0.6331	0.0474	0.620	0.4499	0.390
		Upper	189	-0.0275	0.5372	0.0591	0.512	0.3616	0.590

*Note:* This table presents the results of Generalized Pareto Distribution (GPD) goodness-of-fit tests for extreme value modeling of standardized residuals from three GARCH-family models (EGARCH, GARCH, and GJR-GARCH) applied to the four stock market indices. The tests evaluate whether the GPD adequately models the exceedances beyond the 10% threshold in both tails. The Cramér-von Mises ( $W^2$ ) and Anderson-Darling ( $A^2$ ) test statistics assess the distributional fit, with p-values above 0.05 indicating adequate fit. All tests pass at the 5% significance level except for one case (EGARCH model for S&P 500 lower tail in the Cramér-von Mises test, marked with \*), suggesting that the GPD provides an appropriate model for the tail behavior of standardized residuals across all indices and GARCH models.

### B.3 GPD Tail Fits

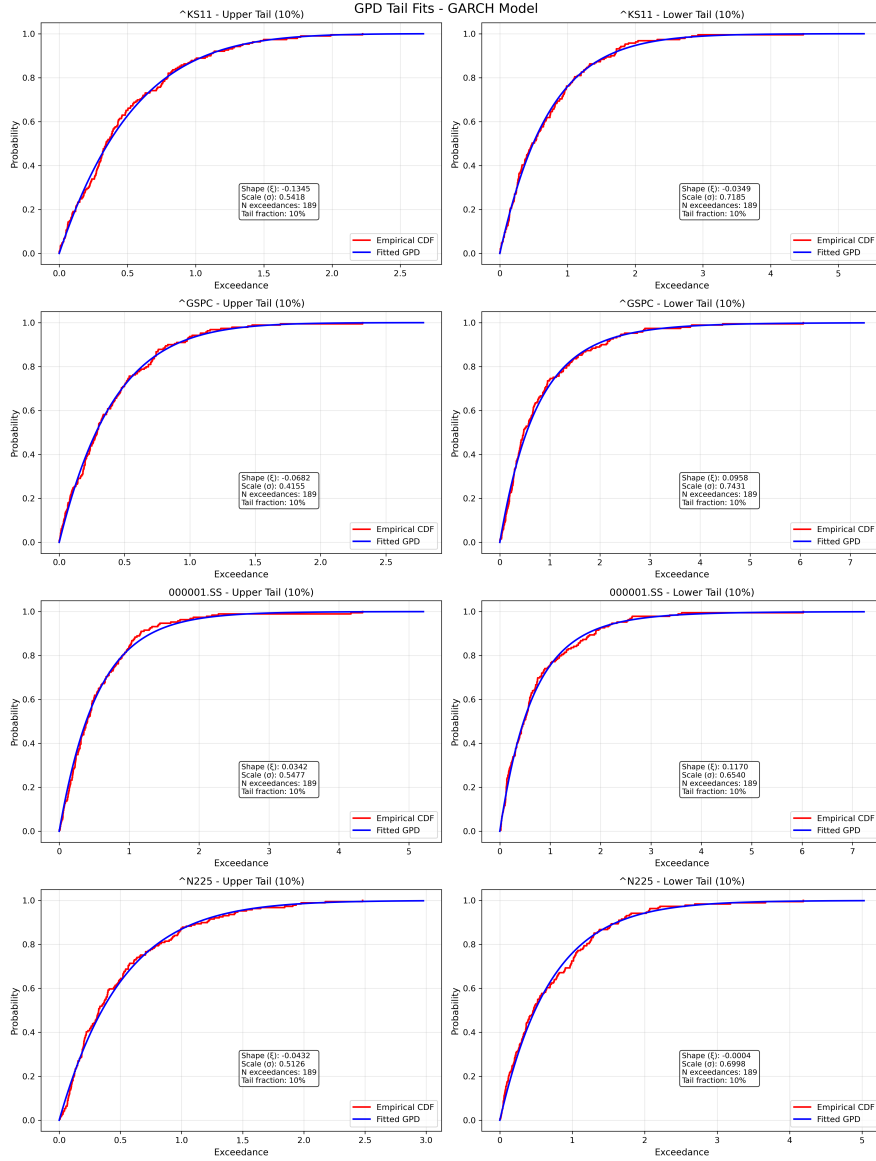


Figure 7: GPD Tail Fits for GARCH Model

Note: Empirical CDFs (red) versus fitted GPD CDFs (blue) for exceedances in upper and lower 10% tails across four market indices. The close fit validates the GPD specification for extreme value modeling.

## B.4 GPD Fit

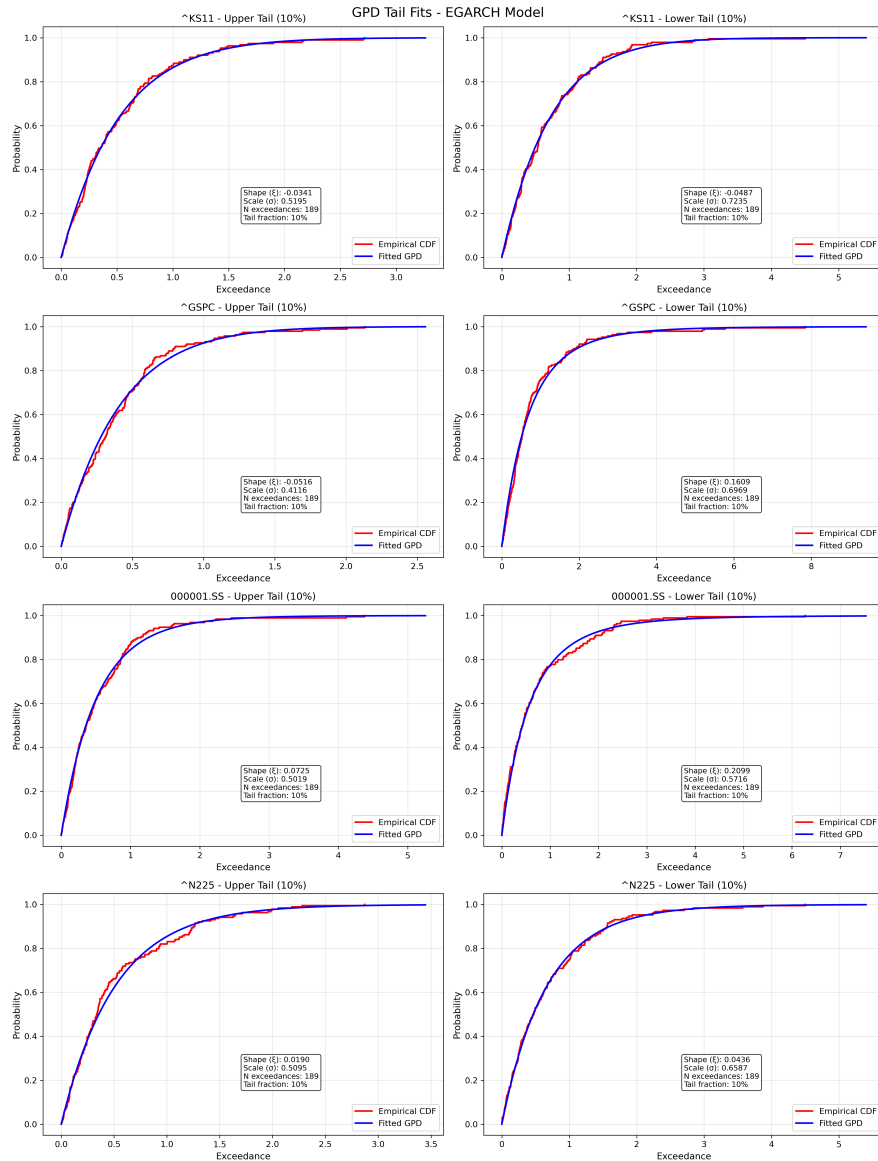


Figure 8: GPD Tail Fits for EGARCH Model

Note: Empirical CDFs (red) versus fitted GPD CDFs (blue) for exceedances in upper and lower 10% tails across four market indices. The close fit validates the GPD specification for extreme value modeling.

## C Copula

### C.1 D-vine Copula Estimation

Table 12: D-Vine Copula Estimation Results

Model	Tree	Pair	Copula Type	Parameters		$\lambda_L$	$\lambda_U$
				$\theta/\rho$	$\nu$		
EGARCH	Tree 1	S&P 500-Nikkei	Gumbel180	1.123	—	0.144	0
		SSE-KOSPI	Gumbel180	1.255	—	0.212	0
		KOSPI-Nikkei	Student	0.548	7.315	0.189	0.189
	Tree 2	S&P 500-KOSPI Nikkei	Frank	0.710	—	0	0
		SSE-Nikkei KOSPI	Gaussian	0.124	—	0	0
	Tree 3	S&P 500-SSE KOSPI,Nikkei	Frank	0.249	—	0	0
	Tree 1	S&P 500-Nikkei	Gumbel180	1.131	—	0.152	0
		SSE-KOSPI	Gumbel180	1.260	—	0.214	0
		KOSPI-Nikkei	Gumbel180	1.579	—	0.319	0
GARCH	Tree 2	S&P 500-KOSPI Nikkei	Frank	0.720	—	0	0
		SSE-Nikkei KOSPI	Gaussian	0.124	—	0	0
	Tree 3	S&P 500-SSE KOSPI,Nikkei	Frank	0.225	—	0	0
	Tree 1	S&P 500-Nikkei	Gumbel180	1.121	—	0.141	0
		SSE-KOSPI	Gumbel180	1.257	—	0.213	0
		KOSPI-Nikkei	Student	0.547	7.531	0.185	0.185
	Tree 2	S&P 500-KOSPI Nikkei	Frank	0.702	—	0	0
		SSE-Nikkei KOSPI	Gaussian	0.122	—	0	0
	Tree 3	S&P 500-SSE KOSPI,Nikkei	Frank	0.231	—	0	0

Note: To examine sequential market linkages, D-vine copula is employed for all three GARCH models. Asset indices: 0 = KOSPI, 1 = S&P 500, 2 = SSE, 3 = Nikkei.  $\lambda_L$  and  $\lambda_U$  denote lower and upper tail dependence coefficients. For Gumbel180:  $\lambda_L = 2 - 2^{1/\theta}$ . For Student:  $\lambda_L = \lambda_U = 2t_{\nu+1}(-\sqrt{(\nu+1)(1-\rho)/(1+\rho)})$ . Gaussian and Frank copulas have zero tail dependence.

## References

- Aas, K., Czado, C., Frigessi, A., and Bakken, H. (2009a). Pair-copula constructions of multiple dependence. *Insurance: Mathematics and Economics*, 44(2):182–198.
- Aas, K., Czado, C., Frigessi, A., and Bakken, H. (2009b). Pair-copula constructions of multiple dependence. *Insurance: Mathematics and Economics*, 44(2):182–198.
- Balkema, A. A. and De Haan, L. (1974). Residual life time at great age. *Annals of Probability*, 2(5):792–804.
- Black, F. (1976). Studies of stock price volatility changes. *Proceedings of the 1976 Meetings of the American Statistical Association*, pages 177–181.
- Bollerslev, T. (1986). Generalized autoregressive conditional heteroskedasticity. *Journal of Econometrics*, 31:307–327.
- Chebbi, A. and Hedhli, A. (2022). Revisiting the accuracy of standard VaR methods for risk assessment: Using the Copula-EVT multidimensional approach for stock markets in the MENA region. *The Quarterly Review of Economics and Finance*, 84:430–445.
- Dißmann, J., Brechmann, E. C., Czado, C., and Kurowicka, D. (2013). Selecting and estimating regular vine copulae and application to financial returns. *Computational Statistics & Data Analysis*, 59:52–69.
- Glosten, L. R., Jagannathan, R., and Runkle, D. E. (1993). On the relation between the expected value and the volatility of the nominal excess return on stocks. *Journal of Finance*, 48:1779–1801.

- Gnedenko, B. (1943). Sur la distribution limite du terme maximum d'une serie aleatoire. *Annals of Mathematics*, 44(3):423–453.
- Gumbel, E. J. (1958). *Statistics of Extremes*. Columbia University Press, New York.
- Harvey, A., Ruiz, E., and Shephard, N. (1994). Multivariate stochastic variance models. *The Review of Economic Studies*, 61(2):247–264.
- Hsu, C.-P., Huang, C.-W., and Chiou, W.-J. P. (2012). Effectiveness of copula-extreme value theory in estimating value-at-risk: Empirical evidence from asian emerging markets. *Review of Quantitative Finance and Accounting*, 39(4):447–468.
- Mandelbrot, B. (1963). The variation of certain speculative prices. *Journal of Business*, 36:394–419.
- McRandall, J. and Rozanov, Y. (2012). Tail risk in the financial markets. *Financial Analysts Journal*, 68(4):34–45.
- Nelsen, R. B. (2006). *An introduction to copulas*. Springer, 2nd edition.
- Nelson, D. B. (1991). Conditional heteroskedasticity in asset returns: A new approach. *Econometrica*, 59:347–370.
- Park, K. and Lee, H. (2022). Analysis on asymmetric tail dependence of portfolio returns. *Journal of Insurance and Finance*, 33(1):83–109.
- Pickands, J. (1975). Statistical inference using extreme order statistics. *Annals of Statistics*, 3(1):119–131.
- Sklar, A. (1959). Fonctions de répartition n dimensions et leurs marges. *Publications de l'Institut de Statistique de l'Université de Paris*, 8:229–231.
- Taleb, N. N. (2007). *The Black Swan: The Impact of the Highly Improbable*. Random House, New York.
- Xiao, M. (2024). Data-driven risk measurement by sv-garch-evt model. *arXiv preprint arXiv:2201.09434*.
- Zhang, B., Wei, Y., Yu, J., Lai, X., and Peng, Z. (2014). Forecasting var and es of stock index portfolio: A vine copula method. *Physica A*, 416:112–124.